Stony Brook University

OFFICIAL COPY

The official electronic file of this thesis or dissertation is maintained by the University Libraries on behalf of The Graduate School at Stony Brook University.

© All Rights Reserved by Author.

Spectral Modification of Diffuse Rear Reflector Layers

for Higher Efficiency in Silicon Solar Cells

A Thesis Presented

by

Jason Matthew Shank

to

The Graduate School

in Partial Fulfillment of the

Requirements

for the Degree of

Master of Science

in

Materials Science and Engineering

Stony Brook University

May 2011

Stony Brook University

The Graduate School

Jason Matthew Shank

We the thesis committee for the above candidate for the

Master of Science degree, hereby recommend

acceptance of this thesis.

Dr. Charles M. Fortmann, Thesis Advisor
Professor, Department of Materials Science and Engineering

Dr. Gary P. Halada, Committee
Professor, Department of Materials Science and Engineering

Dr. Jonathan Sokolov, Committee
Professor, Department of Materials Science and Engineering

This thesis is accepted by the Graduate School

Lawrence Martin
Dean of the Graduate School

Abstract of the Thesis:

Spectral Modification of Diffuse Rear Reflector Layers

for Higher Efficiency in Silicon Solar Cells

by

Jason Matthew Shank

Master of Science

in Materials Science and Engineering

Stony Brook University

2011

Global climate change and energy cost are two of the most important challenges facing modern societies. Solar photovoltaic energy production is one of the most promising avenues by which to address these problems. However solar photovoltaic energy is still too expensive relative to other technologies despite over thirty years of advancement. The work described in this thesis involves improved means for the trapping of light in solar cells and has broad application to almost all existing photovoltaic platforms including silicon (over 95% of all photovoltaic generation is silicon-based). In particular titanium oxide diffuse rear reflector systems were examined to determine the gains possible relative to the non-reflector and planar mirror rear reflectors presently in popular use. The preparation procedures and materials used were chosen for cost competitive advantage. The rear contacts of commercially obtained silicon solar cells were chemically removed and alternative contacts applied. The resultant solar cells were measured using a calibrated simulated solar illumination and the quantum efficiency measurement as a function of wavelength was determined. Significant gains in solar cell long

wavelength spectral response were found when diffuse rear reflector contacts were applied. For example, the quantum efficiency of a solar cell with a diffuse rear reflector peaked at 29.4% at 1100 nm as compared to 12% for a non-reflective rear contact and 14% for that for the case of the as-received commercial solar cell. Work to further improve the diffuse rear reflector is expected to generate even greater gains.

Dedicated to my mother, who over the years has become the heartbeat to my success; and to the memory of my father, whose strength and character has always been an inspiration in my life.

Table of Contents:

List of Figures viii

Acknowledgements ix

I. Solar Cell Theory 1

1.1 Historical Perspective 1

1.2 Photon Scattering 2

1.3 Photogeneration of Charge Carriers 5

1.4 Solar Cell Composition 6

1.4.1 Contact Layer 7

1.4.2 Scattering Layer 7

1.5 Diffuse Rear Reflectors 9

1.6 Spectral Modification 11

II. Experimental Methodology and Techniques 12

2.1 Procedural Methods 12

2.1.1 Contact Layer Etching 12

2.1.2 Contact Layer Application 13

2.1.3 Scattering Layer Application 13

2.1.4 Back Layer Application 15

2.1.4.1 Physical Vapor Deposition 15

2.1.4.2 Vacuum Coating 16

2.2 Testing Methods 17

2.2.1 Simulated Solar Illumination 18

2.2.2 Quantum Efficiency 18

2.3 Doping Profile ……..……..…….. 19

2.3.1 EBIC ……...…….……...……. 20

III. Results and Discussions ...……..…….. 25

3.1 Preparation Results ...…...…….……... 25

3.2 Silver Paste Series ...…… 31

3.3 Aluminum Backing Series ...……...……...…. 36

3.3.1 Temperature Changes …….……. 36

3.3.2 Addition of Materials …….…….. 37

3.3.2.1 Introduction of Strong Raman Shifting Particles …...…….. 38

3.4 Titanium Contact Series …….……. 42

3.4.1 Titanium Results …….....……. 44

IV. Conclusions ……..…….……...…… 46

4.1 Cell Comparison ……...…….. 46

4.2 Improvements and the Future of Diffuse Rear Reflectors ……..…… 47

References …...……...…….. 49

Appendix 1: Optical Layers and Materials for Next Generation Solar Cells ...……...…… 51

List of Figures:

Figure 1: Band Gap Diagram of Silicon Solar Cell ……..……..…. Page 4

Figure 2: Reflectance as a Function of Wavelength for Normal Incident Light ……... Page 8

Figure 3: Sputtering process achieved by the Denton Vacuum Coater …….. Page 17

Figure 4: Unmodified Solar Cell Cross-Section ……...……..…… Page 19

Figure 5: EBIC as a Function of Beam Position ……. Page 21

Figure 6: EBIC Geometry ……...…… Page 22

Figure 7: EBIC Image of Boron Doped Silicon ……...…….…….. Page 23

Figure 8: EDAX Spectrum of Bi-based Back Layer……..……..…… Page 26

Figure 9: SEM Image of the Bi-based Pigment in an Organic Matrix …… Page 27

Figure 10: 40x Bare Silicon ……..……..…… Page 28

Figure 11: 40x TiO_2 Coating ……..……. Page 29

Figure 12: Ag Particles Before Heat Treatment …….....…...…… Page 30

Figure 13: Ag Particles After Heat Treatment .....……..…….…… Page 31

Figure 14: QE Improvement of Solar Cell with Diffuse Rear Reflector ……..... Page 33

Figure 15: Comparisons in Solar Cell Layers ……..……..…… Page 35

Figure 16: Cell Comparison Under QE …….……. Page 39

Figure 17: Solar Simulation Comparison of Raman Shifting Particles …….. Page 41

Figure 18: Quantum Efficiency of Si Cell with Ti/Al Backing……... Page 43

Figure 19: Solar Simulation of Si Cell with Ti/Al Backing …….…….. Page 44

Figure 20: Quantum Efficiency Comparison of Ti-Based Si Cells ……. Page 45

Acknowledgements:

I gratefully acknowledge the invaluable support and encouragement of my advisor, Dr. Charles M. Fortmann, who has set an example through which I have developed an understanding, appreciation, and love for conducting research. I thank him for dedicating countless hours in which I was given priceless guidance and suggestions. I also appreciate the pleasant conversation from time to time about past experiences during life's journey.

I would like to thank Mr. Eric Laufer and Mr. Marc Dee for their support towards the research of our group. Their efforts in contributing the necessary equipment and supplies to the entire research group cannot be more appreciated. It is a great feeling to gain an industrial mindset while working in an educational setting; you both have gone above and beyond to provide that.

I would like to acknowledge Dr. Andrzej Lipski for being extremely generous in his time to deposit aluminum on the back of several silicon cells in the beginning of my research. His help provided a huge stepping stone towards the progress and completion of my topic for this thesis. I would like to also thank Dr. Jonathan Sokolov and Dr. Gary Halada for accepting my request to serve on my committee, as it is much appreciated. I have thoroughly enjoyed your classes and your assistance to my learning.

I would also like to acknowledge Dr. Jim Quinn for his time and dedication in helping me with various appointments to use the SEM. His dedication and time to my learning and growth over both my undergraduate and graduate careers has been extremely appreciated. He has become a dear friend to me and I credit much of my success to our pleasant and intellectual conversations over the years. I would also like to thank fellow graduate students Joseph Ortiz and Christopher Young for help with Raman Spectroscopy among other talks and conversation.

I would like to thank the faculty and students of the Materials Science Department for valuable advice and discussions concerning a number of scientific aspects. I would also like to extend a personal thank you to the members of our solar group for their

advice and pleasant conversation. Yeona Kang, Mikael Marra, Ping Lee, and Komal Magsi; you have all become dear friends of mine.

Finally I would like to acknowledge the love and support of my mother, who has given me wings of strength to fly into life; you have never failed to be my hero. I would like to acknowledge my entire family, especially my grandparents, whose beliefs in my abilities have advanced me far. I express my appreciation and delight for my many close friends of "the crew" for always being there during the times when things weren't going so well, but also when things couldn't be better. I also thank Emily McMahon for being the special person in my life to turn sorrow and frowns to happiness and smiles. Your art is an inspiration for me to work hard towards my goals and never give up, as your words and support have also motivated to me to do great things. I am so incredibly lucky to have met you; you will never know how truly special you are to me.

I. Solar Cell Theory

1.1 Historical Perspective

A discussion of electrical force and work begins with the basic unit of electrical energy; the volt. The volt is named for the Italian physicist Alessandro Volta who in 1800 created the first electric cell[1]. His discoveries have driven almost two hundred years of improvement in electrical devices, batteries, and have also created the basic theory of solar cells; that the presence of light can create a voltage. It took a number of years before light energy could be converted to electrical energy.

French physicist A.E. Becquerel advanced Volta's work when in 1839 he discovered the conversion of light energy into electrical energy. This phenomenon became known as photovoltaic effect, meaning "light" and "voltage"[2], paving the way for Charles Fritts in his creation of the first photovoltaic cell in 1883. Although the efficiency of this first cell was only 1%, it demonstrated that light could indeed be converted into electrical power. The composition of the cell consisted of a selenium semiconductor coated with a thin layer of gold to form an electrical junction[2]. His work later provided Russian physicist Aleksandr Stoletov with the groundwork he needed to build the first practical photoelectric cell in 1888[3]. Later photovoltaics took another giant step towards industrialization when Albert Einstein explained the photoelectric effect in 1905. For this, he won the Nobel Prize in Physics in 1921[4].

After Russel Ohl's inventing and patenting of the first modern junction semiconductor solar cell in 1941[2], three workers at Bell Laboratories in New Jersey developed the first silicon photovoltaic cell in 1954. Daryl Chapin, Calvin Souther Fuller, and Gerald Pearson used a

diffused silicon p-n junction to show how silicon absorbs photons and creates a voltage[5]. All of this has been vastly improved and optimized to current state of the art megawatt solar power generating plants, located throughout the world[6]. Also in production is the more advanced multi-junction silicon cell (albeit with applications be limited by the high manufacturing cost).

Silicon solar cell functionality relies on the boundary interface of a p-n junction. Further solar advancements has also allowed for interest in multi-junction solar cells in which the solar cell has multiple p-n junctions. By use of this technology, more use of the solar spectrum is used, thus enabling the creation of more power. Although this thesis did not investigate multi-junction silicon cells, it is worth mentioning due to the importance they have in the development of photovoltaics.

1.2 Photon Scattering

Photon absorption and scattering are two important considerations for solar cell efficiency. The greater the number of photons absorbed within the solar cell absorber layer the greater the current and efficiency of the cell.

One method of strategy for increasing the number of photons absorbed in a solar cell is to use a mirror-like rear reflector combined with a rear electrical contact. The mirror will reflect any unabsorbed photons back into the cell for a second chance at being absorbed. A properly designed diffuse rear reflector can further increase photon absorption probability by increasing the angle at which light is scattered. Large angles lead to longer path lengths through the solar cell (and therefore increased absorption probability) and also lead to total internal reflection at the solar cell front surface leading to vastly increased photon path lengths and increased

absorption probability. However, the number of photons that are geometrically scattered within a diffuse rear reflector must be viewed as a transparent bulk-light scattering layer, thus presenting the task of index matching. This is further discussed in section 1.3.

The physical relations between photon energy (E) and wavelength (λ) of a given photon are defined by[7]:

$$E = \frac{hc}{\lambda}$$

where h is Planck's Constant (6.63×10^{-34} J · s) and c represents the speed of light (3×10^{8} m/s). In visible light, photons have wavelengths between 400 and 700nm. Since solar irradiance peaks in the visible spectrum, eye sight and most photovoltaic solar cells are tuned to these wavelengths. However, silicon, the most widespread installed solar cell, has a maximum response to approximately 1100nm. Therefore, this work examines the response from 300 to 1100nm, which includes the range at which silicon absorbs light.

Photon energies increase with decreasing wavelength[7]. Most solar cells cannot convert any extra energy above the band gap into electrical power. Therefore, blue light photons, although having more energy than yellow light, produce the same energy per photon in silicon solar cells. The same can be said about the relationship between increasing wavelength and decreasing energy. Therefore, it is necessary to learn how to decrease wavelength while containing enough photons to increase energy as well.

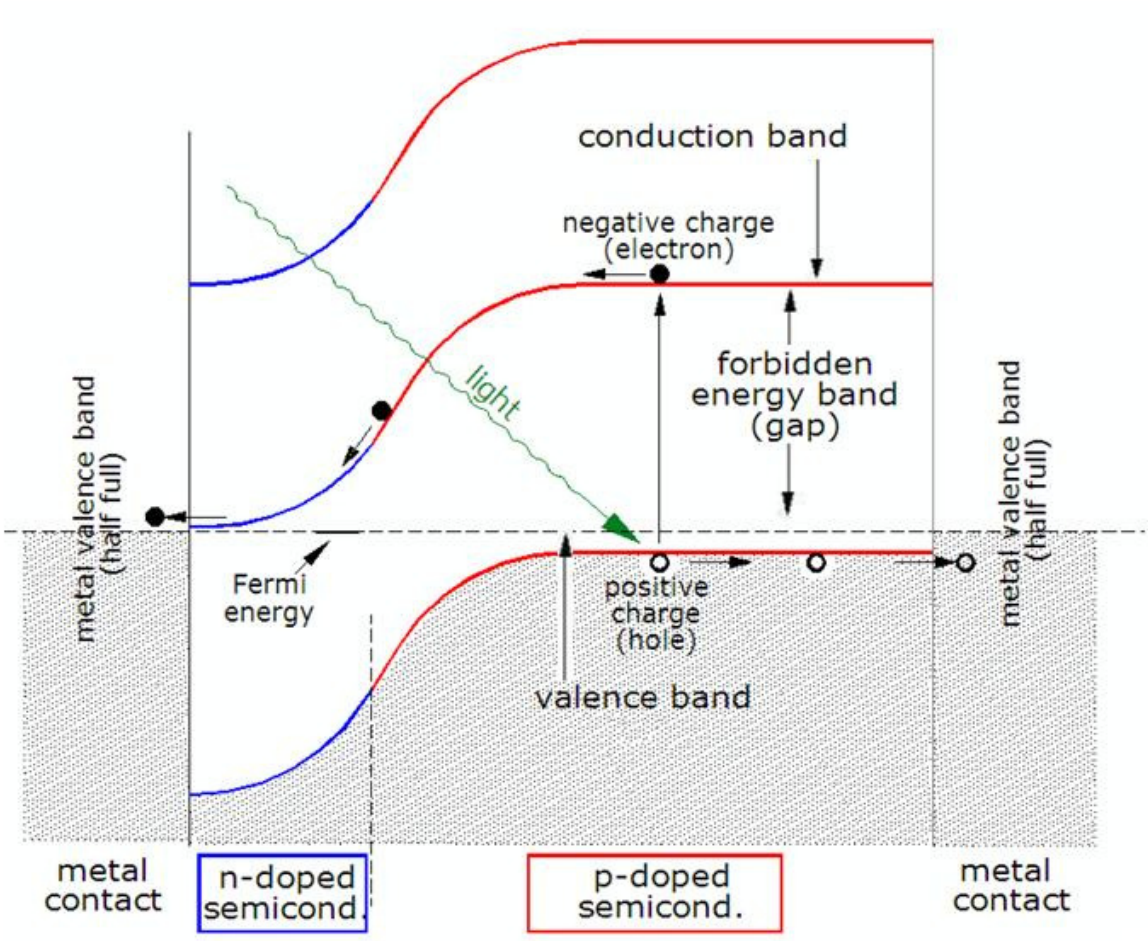

Figure 1: Band gap diagram of a silicon solar cell, showing the path of a photon (light) and resulting direction of an electron after collision[8].

1.3 Photogeneration of Charge Carriers[9]

Photons incident upon a solar cell may be reflected at the front contact due to refractive index change. Photons with the energy less than the band gap of the solar cell pass straight through the silicon without absorption. The refractive index and reflectivity are related at normal incidence to the coefficients of reflectivity (r(ω)) and extinction (K(ω))[10]:

$$r(\omega) = \frac{n+iK-1}{n+iK+1}$$

The refractive index can be determined through a number of methods such as ellipsometry. In principle one could simply use the above equation with measurement of the relative ray angles created when a light beam travels from a known refractive index material to an unknown material (however, this is seldom done).

From a solar energy point of view, the most desirable outcome for incident photons is absorption by the silicon and generation of an electron–hole pair. However, this is only possible if the photon energy is higher than the band gap value of silicon. If this outcome takes place, it is possible for the photon energy to be converted to electrical energy. Photon absorption occurs when a photon transfers its energy to the electron which is thereby promoted from the valance band to the conductive band as seen in figure 1, which also shows the process of photogeneration of charge carriers[8].

Excess energy beyond that needed to promote the electron from the valence band to the conduction band is converted into heat[9]. In a single band gap solar cell, the cell suffers limited efficiency due to the inability to convert a majority of the photon energies in the solar spectrum,

let alone the broad range of them. As previously mentioned, photons below the band gap of silicon, or the cell material in general, are wasted since these photons cannot be absorbed. For the above gap energy photons, the only energy utilized is that which is necessary to generate the electron-hole pair with the remaining energy being converted to heat[12].

Multi-junction solar cells due to systematically stacked band gaps better convert each portion of the solar spectrum. They can consist of several materials including silicon, germanium, and gallium-arsenic; however, these are expensive. This work focuses on optical structures that can help single junction solar cells better collect light. These structures include index and near-index matched diffuse rear reflectors and rear reflectors with the capacity to modify the incident spectrum in a manor favorable to photogeneration and electrical power generation.

1.4 Solar Cell Composition

A cross-section of a modern silicon solar cell can be seen to be comprised of several optimized layers fused together. Components include a grid contacts used on the front and mirror-like metal contacts on the rear. The grid contact is designed to efficiently collect electrons from the thin highly doped layer. Typical commercial solar cells employ an anti-reflection coating (ARC), which reduces light losses due to reflection. It may also increase stability. The choice of material for an ARC ranges between several, including SiO, SiO_2, Ta_2O_5 or the preferred choice of TiO_2. All of these are particularly good for their high UV transmission. Ultimately, reflectivity decreases from greater than 15% to less than ~ 3%[13]. An efficient ARC strategy such as surface light scattering structures also produces light paths that are not

perpendicular to the junction interface[13]. Figure 2 shows the response of several Si cells including the Comsat nonreflective (CNR) cell.

1.4.1 Contact Layer

Photons absorbed in the top-most layers of highly doped silicon usually do not produce much power because the recombination is very short in these doped layers and the electrons do not live long enough to diffuse to the appropriate contact. In theory, the minority carrier of the electron-hole pair diffuses towards the junction where it will be collected and transferred to the electrical contact.

1.4.2 Scattering Layer

The concept of light scattering within the cell is instituted to maximize the path length that a photon travels within the solar cell to maximize the probability of absorption. A TiO_2 diffuse rear reflector is a useful material for this task. Although it is not as conductive as a mirror-like metal, it serves as an excellent scatterer and reflector for light[14].

In the thin-film solar cell case, a rough tin-oxide coated solar substrate provides a front contact with an increased light scattering ability. However, a TiO_2 diffuse rear reflector can increase the current of optically thin amorphous Si-based solar cells beyond that of using a TCO (thin conducting oxide) glass substrate[14]. Light scattering allows thinner more cost effective solar cells to be made.

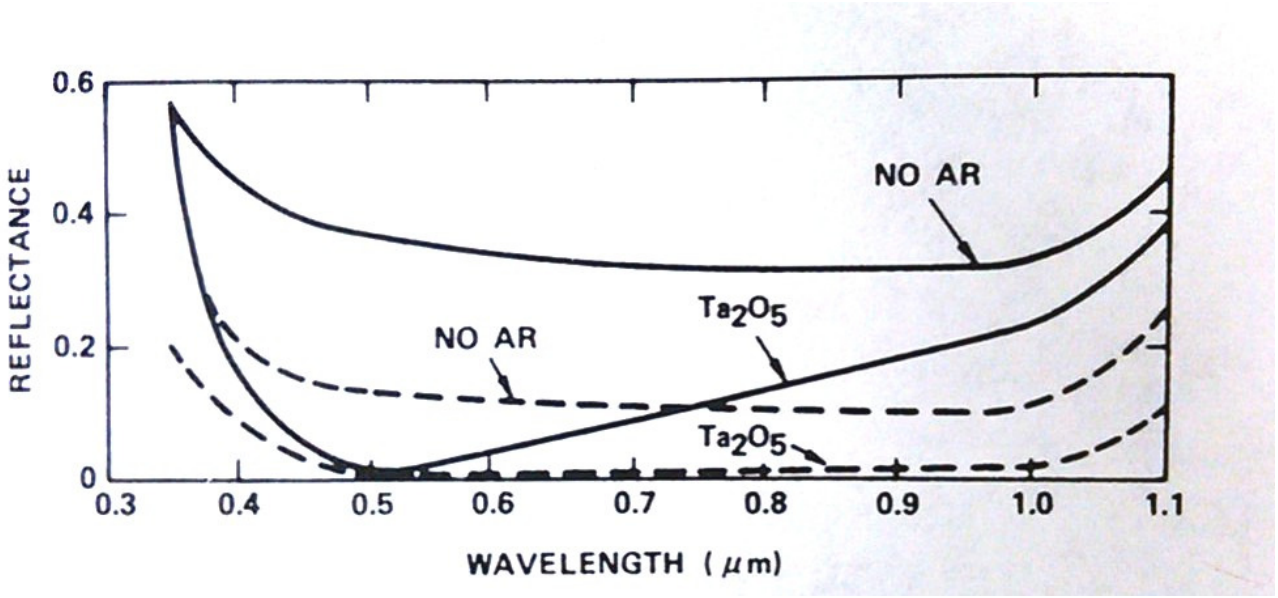

Figure 2: Reflectance as a function of wavelength for normal incident light[13].
(Upper and lower solid curves) Flat, polished Si Surface without and with quarter-wave AR coating (Ta_5O_3), respectively.
(Upper and lower dashed curves) CNR texturized surface without and with quarter-wave AR coating (Ta_5O_3), respectively.

1.5 Diffuse Rear Reflectors

One must consider the important concept of light trapping, which allows for the most efficient absorption of light by a given solar cell system. One of the downfalls of a Si-based solar cell is its relatively low band gap energy of 1.1eV and weak absorption of light due to the indirect band gap of silicon[13]. Overcoming the relatively low weak absorption of light in the solar spectrum near or below the Si band gap are areas that may need further optimization.

The advantage that diffuse rear reflectors offer is the ability to scatter light at sufficiently large angles (See Appendix 1). This therefore increases the probability of the total internal reflection at the front surface, allowing much longer light path lengths within the solar cell absorber layer when compared to a simple mirror like rear reflector[14]. The diffuse rear reflector must also have a large refractive index as previously noted by Winz *et al* in order to obtain large scattering angle within a high index solar cell (refractive index of silicon > 3.4) [14]. More information on solar cells using diffuse rear reflectors can be found in Appendix 1.

The use of a diffuse rear reflector allows for the reflection at angles large enough for total internal reflection when light is incident on the front system after passing through the cell. They offer the advantage of scattering light to sufficiently large angles, increasing the probability of total internal reflection at the front surface[15]. Therefore much longer light path lengths within the solar cell absorber layer exist when compared to a simple mirror like rear reflector. Nonetheless, three main benefits support the use of a diffuse reflector near band-gap light[14]. First, the reflection of non-absorbed light back through the silicon layer allows for re-absorption as well as greater use of the light and less waste. Second, the average distance traveled through a Si layer increases due to the oblique angle at which reflected light travels. Third, the total internal

reaction into a thin Si layer causes a fraction of the diffuse light reaching the front surface to be reflected again.

It is important to note that if the diffuse rear reflector is insulating, then it must be used in conjunction with conductive elements. Also, the refractive index must be close to that of silicon as possible (silicon has a refractive index of approximately 4). Several materials can be used to serve as a diffuse rear reflector, however the aforementioned material used for the work in this thesis is titanium dioxide (TiO_2). TiO_2 serves as an excellent scatterer of light, has little absorption in the spectrum needed by the solar cell, and it very cost effective.

To produce a contacting layer, Al must be diffused into the silicon. The rear contact layer is typically ~5μm thick in the silicon solar cell case[13]. Since Al is a p^+-type dopant in silicon, Al can be used to create a contact layer when a p^+-type silicon absorber is used. Typically, this contact layer is produced by diffusing metallic Al into the silicon for an appropriate time period at an appropriate temperature. This work experimentally examined Al contact and Al diffused contacting regions for use with diffuse rear reflectors. The work-function of the metal contact must also be well matched to the silicon and its majority carrier type. Considering a concentration field associated with silicon, several quantities are considered including the diffusion coefficient (D), time of diffusivity (t), and distance of diffusivity (x) into the silicon image field. This is included in the concentration field formula[16]:

$$C(x,t) = C_0 \, erfc\left(\frac{x}{2\sqrt{Dt}}\right)$$

The main point of interest is the distance into the silicon at which Al concentration exceeds ~10^{19}/cm^3; the concentration needed to make an effective concentration layer. The time of diffusivity can be identified as the time the sample is at a constant temperature in the furnace, while the diffusion coefficient of Al in silicon is[17] 8.0 cm^2/sec. The solution to Fick's 2nd law, also referenced as the linear diffusion equation, is a linear second order partial differential equation. However, in its integral form, Fick's 2nd law for diffusion is[16]:

$$erfc\,(z) = 1 - \frac{2}{\sqrt{\pi}} \int_0^z e^{-t^2}\, dt$$

While the equation for concentration field covers a macro-scale of diffusion, the equation for hop distance represents diffusion on a micro-scale. Calculating the number of hops and the hop distance will also satisfy the need for knowing the distance the Al dopant has diffused.

1.6 Spectral Modification

Luminescent and Raman scattering structures within the diffuse reflector may offer the ability to be spectrally modified by up- and down-converting sunlight[14]. This presents a means by which to scavenge and convert unused light into light of sufficient energy and therefore broaden the conversion range. Although Raman scattering is an intrinsically weak property often used for material characterization, it can account for a significant loss (~25%) in long distance fiber optic communication.

II. Experimental Methodology and Techniques

2.1 Procedural Methods

Commercial grade operational solar cells with efficiencies of ~14% were employed for rear contact investigation. Procedures were developed for the removal of the as-supplied rear contact while new diffuse rear reflectors were prepared and tested under the conditions reported in section 2.2.

2.1.1 Contact Layer Etching

The as-supplied silicon cells were coated with a proprietary gray back layer involving initial experiments to be focused on the removal of this rear contact. Various paint removers and solvents were tested to determine if these could safely remove the as-supplied contact. The goal was to remove the back contact without disturbing the underlying silicon layers. If the contact could be removed without etching the highly doped silicon contact layer, there would be no need to form a new contact layer. Unfortunately, the commercial grade paint removers and solvents were unable to successfully remove the back contact, providing the need for a new etching method.

Several acid etches were used in the next attempt to remove the back contact, including the use of a mixture of H_2SO_4 & nitric acid. Also used was an immersion of the cells in a heated mixture of 4:1 nitric acid to sulfuric acid. However both of these mixtures failed to produce significant removal of the as-supplied contact. Further tests included the use of EDAX (Energy

Dispersive X-ray Spectroscopy), Raman Spectroscopy (see Appendix 1), and SEM (Scanning Electron Spectroscopy). The results of these are presented in section 3.1.

The acquired data and presented work shows the successful etching of the contact. The proper cleaning of the cell in a hydrofluoric acid /DI water mix will complete the etching and present a bare Si solar cell. New diffuse rear reflector layers can now be deposited to allow for testing to be done on the modified cells.

2.1.2 Contact Layer Application

After a complete etching of the contact, the application of a new contact layer is important in providing a replacement p^+-layer and establishing a conductive path for electron travel. Since the contact layer must be conductive, the best solution for this is to use a metal, most specifically aluminum due to its outstanding conductive properties. The contact layer of aluminum must be thin enough to be unable to absorb light. Therefore a 40Å layer of aluminum was evaporated onto the back of the silicon by method of PVD (see section 2.1.4.1). Later on, this layer was then lowered to 20Å after the ability to apply precise thicknesses was acquired. After application of the contact layer, an attempt to drive the newly coated layer into the silicon to create a highly doped contact layer was done by heat treating the sample at 500° C. After removal from the furnace and a careful inspection, the next step can be taken.

2.1.3 Scattering Layer Application

Application of a scattering layer requires the mixture of several key components that creates a layer of material specifically for light scattering. From work with Dye-Sensitized Solar Cells (DSSC's), a TiO_2 mixture has shown outstanding abilities to scatter light. Therefore, a TiO_2 mixture was prepared and sprayed onto the cell after application of the contact layer is complete.

These TiO_2 mixtures were composed of 2.5 ml of acetic acid and 6 ml of 2-propanol per 0.5g of TiO_2 powder. The contents were then mixed and grinded with a mortar and pestle until the substance resembled skim milk. Using a pipette, the contents were placed in a spray bottle, which was then attached to a hobby sprayer. For rigidity, the cell was taped to an 8x8 square of cardboard. It is important that the edges of the cell are taped completely so that conductive paths were not created around the solar cell.

Once the spray was dry, the tape was carefully removed to reveal a uniform coating on the back of the cell. The cell was heat treated again at 500°C for 30 minutes, increasing to the set temperature over a time period of 30 minutes. Doing this allowed for fusion of the TiO_2 particles and decrease of the amount of existing gaps for photons to pass through. Overall, the baking process used lasted approximately four hours, which included heat up, baking, and cool down phases. The cell was then removed and stored for a final phase of PVD (if needed). Similar methods are described in Appendix 1.

2.1.4 Back Layer Application

The final step in completing the modification of the cell is the recoating of the cell with a back layer. Two methods were used to deposit a back layer onto the cell. The first method used was painting a thin layer of silver paste onto the cells. After drying, this layer created a conductive atmosphere as required of all back layers in order for the cell to achieve maximum efficiency. The process of doing this was very simple and similar to that of section 2.1.3, as each edge of the cell was taped to a piece of construction paper taped to a piece of cardboard. The cardboard allows for sturdiness to support the cell and protect it from breaking. A thin but visible layer of the paste was then painted onto the cell, and after drying, the cell was carefully removed and stored until testing was done. The results of these are shown in section 3.1.

The silver paste provided some great results; however the data acquired showed room for improvement. Therefore, methods of PVD and vacuum coating were instituted to apply a more conductive back layer to the cell. Each of these methods required different machines while yielded different procedures and results as well.

2.1.4.1 Physical Vapor Deposition

PVD is a method that deposits a film onto a substrate by evaporating from a source. For this work, Al was typically used. Therefore, small pieces of aluminum were evaporated on the cells to complete the back layer. PVD is useful due to the ability to coat more than one substrate each with a desired thickness.

The PVD process is simple; before starting, the substrates were carefully masked using aluminum foil to protect the top of the cell. The cells were then clipped inside a vacuum chamber. Depending on the desired thickness of the deposited layer, a number of aluminum wire sources were bent and hung from a tungsten wire heating element. These were connected to two electrodes, which were electrically heated to a temperature sufficient for Al evaporation. Once the aluminum source was consumed, the electrical source was cut. After the system cooled, it was vented and the sample was removed. This PVD method proved too difficult to control deposited film thickness and impurity incorporation from the tungsten heating element was apparent. Therefore, a more improved method of Al vapor deposition was desired.

2.1.4.2 Vacuum Coating

A method to more efficiently deposit Al films occurred by use of a commercial sputtering vacuum coater. This differed from the previous PVD method by allowing the samples to rest on a stage inside a chamber, rather than having the samples suspended by clips. When desired, the chamber can be pumped to pressures of 10^{-7} Tor. Coating of the samples occurs via Argon ions sputtering material from a source. As the electrons bombard the material, they kick out atoms of metal within the chamber. The low pressure allows for the coating material to travel from the source to the substrate. The commercial sputtering system used employed a highly accurate deposition monitor so that film thickness could be controlled to ~1Å. When the desired thickness is achieved, the chamber is then vented and sample is removed. An image displaying this process is shown in figure 3[18]. Vacuum coating serves as a much better method than PVD as it requires

less time and also allows for safer conditions for the cell. The vacuum coater used for this work was a Denton Desktop Pro Vacuum Coater.

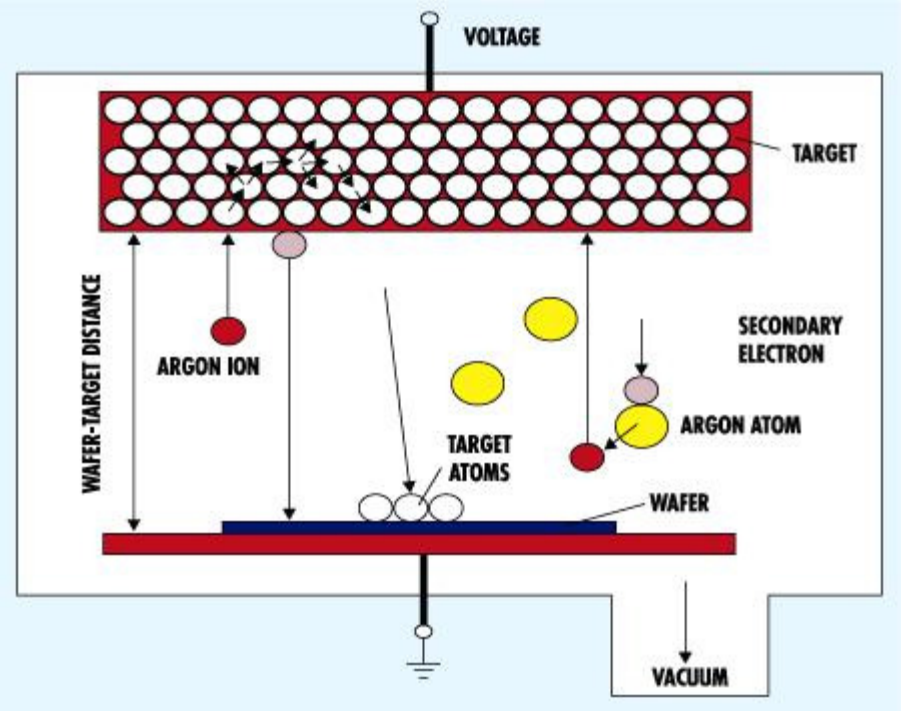

Figure 3 – Argon sputtering process of metal deposition achieved by the Denton Vacuum Coater

2.2 Testing Methods

After completion, all cells were characterized using state-of-art solar simulation and quantum efficiency vs. wavelength measurement. All characteristics included: fill factor, open circuit voltage, short circuit current and QE vs. λ. From the data acquired from these tests and results, necessary improvements on the cells can be determined as improvements are always achievable.

2.2.1 Simulated Solar Illumination

The solar simulation employed a 450 W xenon arc lamp and was run at ~100 mw/cm^2 with a rear AM 1.5 spectrum. The resultant beam was a continuous near 1.5AM solar-like spectrum in a collimated beam[19]. All solar characteristics presented in this thesis were generated using a Newport Oriel Sol1A.

2.2.2 Quantum Efficiency

The efficiency of a solar cell is one of its most important characteristics. The quantum efficiency (QE) is also very important as it determines the probability a given photon of a given wavelength will generate a collected electron-hole pair. This is shown by the equation[20]:

$$QE = \frac{output}{input} = \frac{electrons/sec}{photons/sec} = \frac{(current)/(charge\ of\ one\ electron)}{(total\ power\ of\ photons)/(energy\ of\ one\ photon)}$$

Since various wavelengths get absorbed in different regions of the solar cell, QE can be used to probe these various regions. QE characterization presented here were determined using a Newport Oriel Monochromator model #74125.

2.3 Doping Profile

In solar cell and semiconductor production, doping a sample means to intentionally introduce an impurity to a pure sample for the purpose of regulating the electrical properties to a desired state. Figure 4 shows a cross-sectional image of an unmodified silicon solar cell. The left most portion of the image shows the as-delivered back, while the dark region shows the silicon.

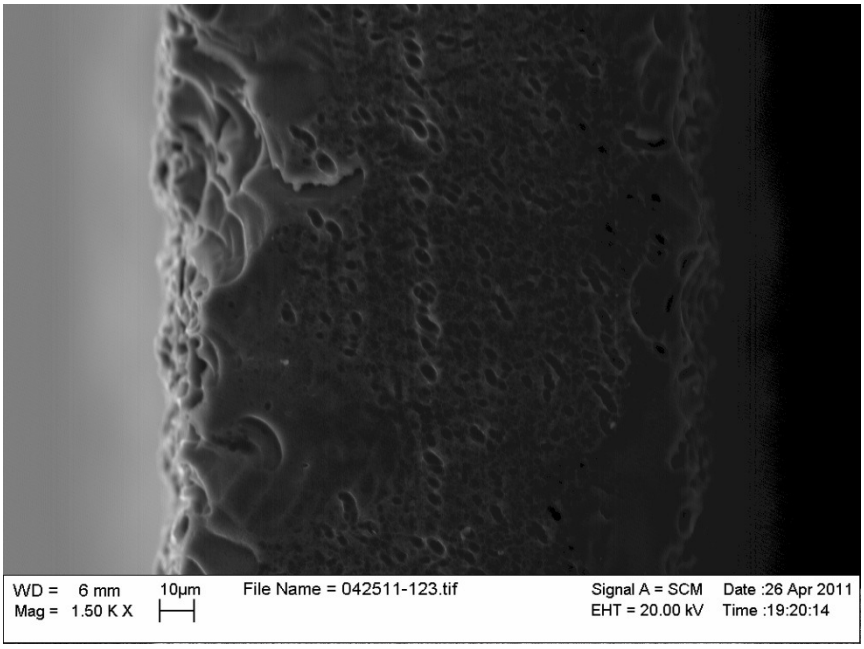

Figure 4 – Cross Section an unmodified silicon solar cell.

The contrast can be used to gain some insight into the electron concentration within the various layers, where the lighter elements have greater electron density. Also, by examining this image, we can further view the distance needed for electron travel, as it clearly shows the full 180µ Si solar cell.

2.3.1 EBIC[13]

In some cases, it is possible to use an electron microscope to image the change generating and collection mechanism of a solar cell. Electron Beam Induced Current (EBIC) directly uses an electron beam rather than a photon to generate charge. Electrons excite very small regions of the sample material. The beam is scanned across the edge of the solar cell to determine collection as a function of x[13]. The collection is given by:

$$I_{sc} \cong A\, exp\,(-x/L)$$

where x is displacement, L is the minority carrier drifts and A is constant. In general, this measurement is insensitive to light trapping because the energy of electrons in an SEM is thousands of times that of a visible photon. Each electron excites thousands of electron-hole pairs. A typical plot showing this effect illustrated by the short-circuit equation can be seen in figure 5, illustrating I_{SC} versus *x* for a p-n junction silicon solar cell[13].

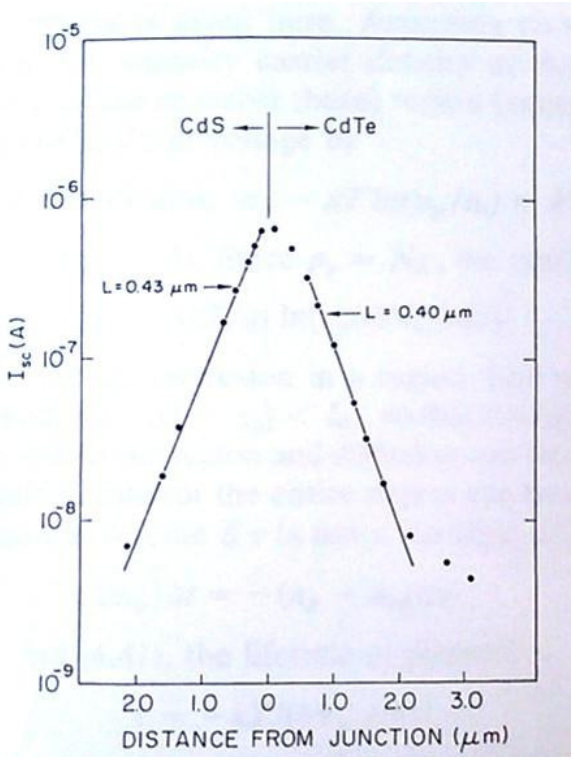

Figure 5: Electron-beam-induced current as a function of beam position for an experimental semiconductor[13].

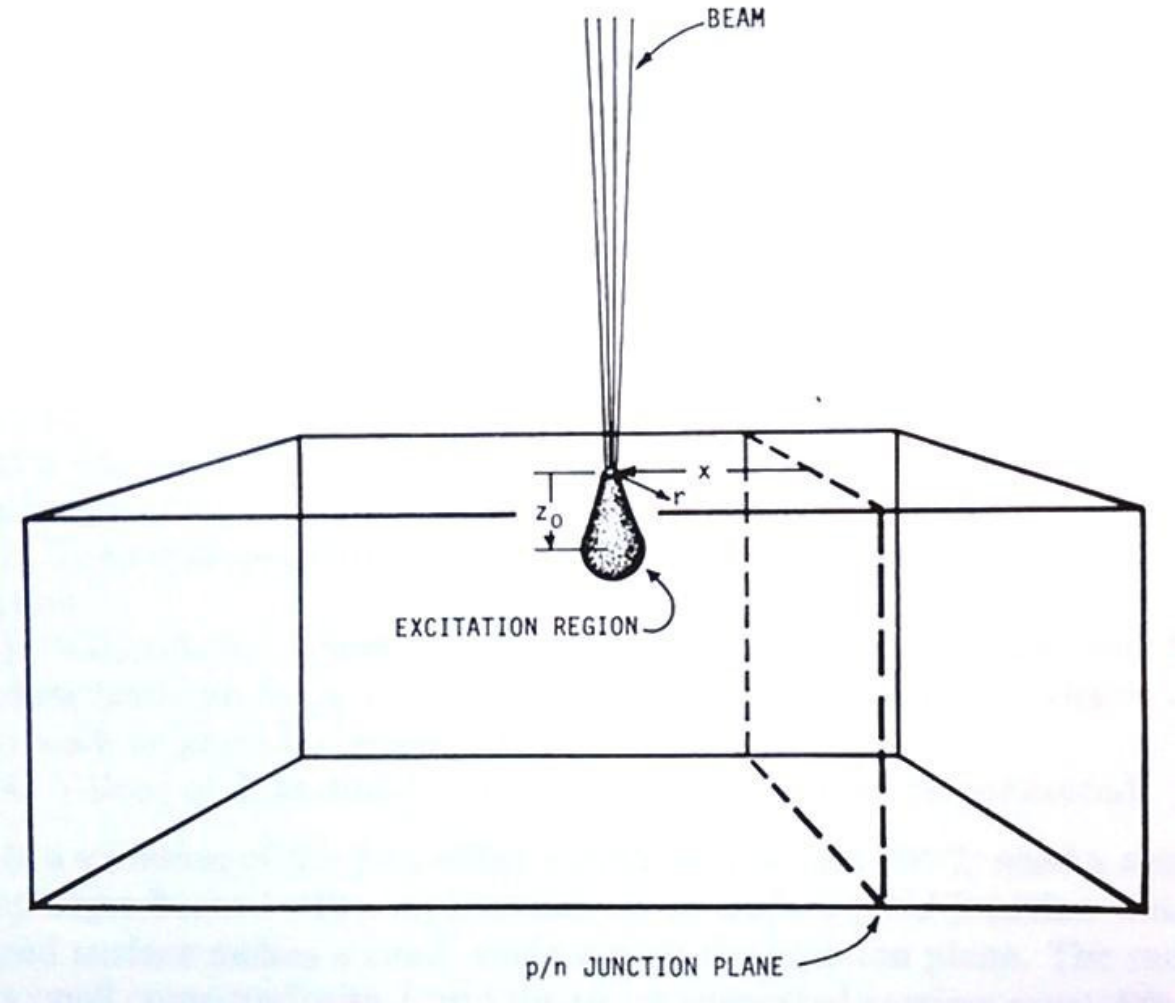

Figure 6: EBIC Geometry[13]

The EBIC method is a favorable choice for illustrating doping profiles due to several advantages that it offers. First, the junction plane can be located with respect to the metallurgical junction. This then proceeds to allow the carrier diffusion length *L* to be conveniently measured. These *L* values can be as small as a tenth to two-tenths microns to be readily measured.

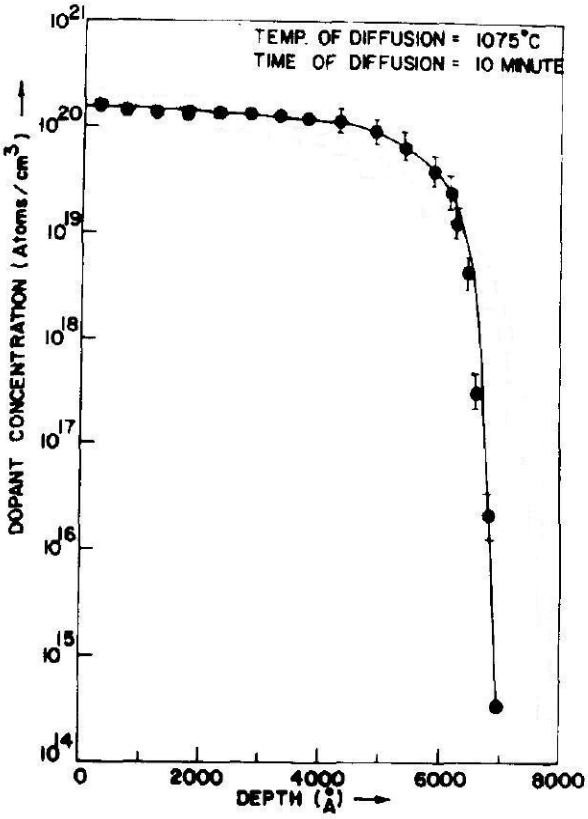

Figure 7 – Doping profile of Boron in Silicon

As seen in figure 7, by using an SEM to bombard a monocrystalline silicon solar cell with electrons, a doping profile can be achieved[21]. One can see that the amount of dopant remains relatively constant until the depth reaches ~6000Å. Although this describes the doping of silicon with boron and not aluminum, this data can still be used in testing the modified cells in this work. EBIC could provide essential knowledge related to diffusion induced aluminum and

dopant profiles. The need for doping will be further discussed, and the reason for doping the crystalline silicon cells will be explained below.

III. Results and Discussion

3.1 Preparation Results

Subsequent research was conducted on the makeup of the as-supplied silicon cells. EDAX (energy dispersive x-ray spectroscopy) analysis of the rear contact revealed large concentrations of aluminum. Research on the removal and etching of aluminum found that aluminum can be naturally etched with a solution of sodium hydroxide (NaOH) and deionized water[22]. Here, solutions consisted of ~4g of NaOH beads dissolved in 20ml of deionized water. The cell was then placed in a small beaker of this solution until the paint was visibly peeling off the cell, or for about one hour maximum. In some cases, remaining contact was gently scraped off.

The NaOH etch produced some unwanted etching deposits on the front surfaces of the solar cell. A commercial product was found to shield the front surface from these unwanted reactions during rear contact removal. Deposits were also noted on the rear silicon surface after contact removal. Tests under EDAX, Raman spectroscopy, and Scanning Electron Microscopy (SEM) were taken to determine the nature of the deposits. A Thermo Nicolet Almega dispersive Raman Spectrometer indicated that these deposits produced several peaks at 960cm^{-1}, suggesting silicon-oxide. Further EDAX testing also revealed the presence of bismuth. Although this may have been an external contamination, research found that bismuth could be removed by potassium hydroxide (KOH) [22]. It was also found that KOH removed several other contaminants that NaOH could not.

Using a solution of approximately 4g of KOH dissolved in 20 ml of deionized water, a small test cell was used to investigate aluminum etching. The front of the cell was not damaged either since the commercial masking agent was not affected by the KOH. Assessing the composition of the back layer was now a concern and resulted in further testing of the residue from the back layer. After etching and scraping the back layer from the silicon cell, the substances were again examined by SEM. The EDAX spectrum of these residues is shown in figure 8.

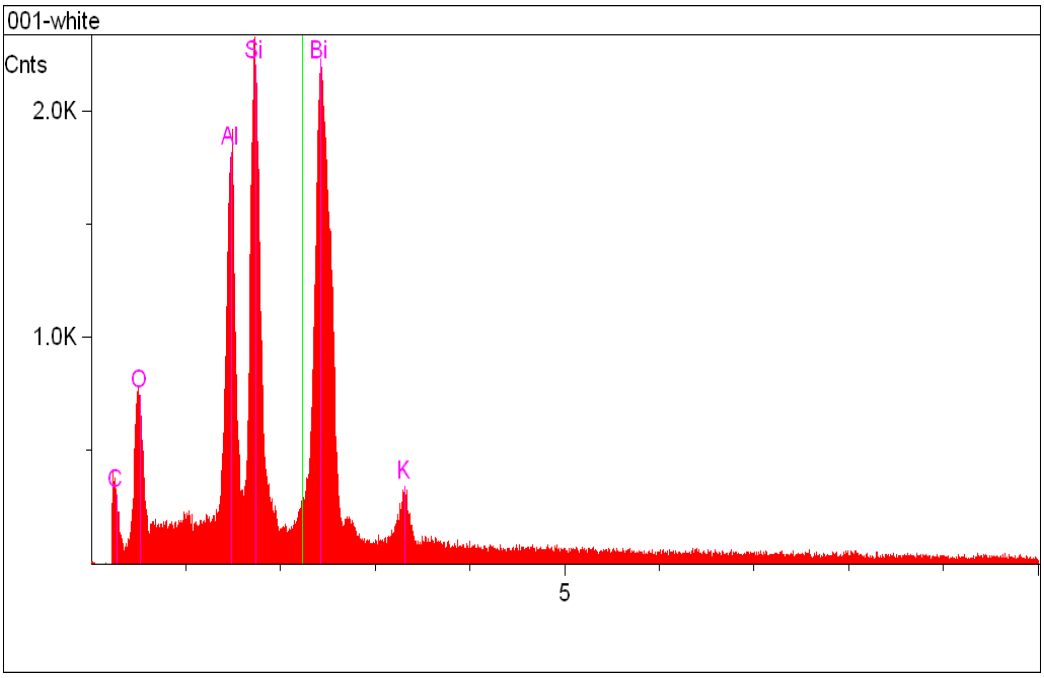

Figure 8 – EDAX spectrum of the bismuth based back layer.

One can see by the peak positions that aluminum, silicon, and bismuth were present. While originally thought to be an Al-based paint, the substance now appeared to be a bismuth-based pigment in an organic matrix. The SEM image also showed an interesting image of the

bismuth particles scattered within the matrix. This can be seen in the image below taken at 10,000x, in which the white particles represent the bismuth within the darker organic matrix.

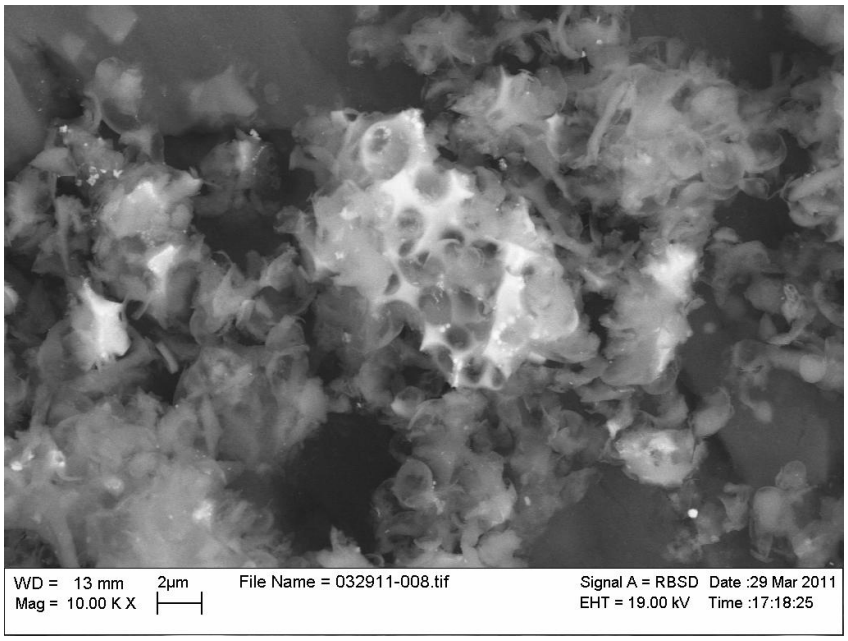

Figure 9 – SEM image of the bismuth-based pigment back layer in an organic matrix.

All subsequent samples were etched with KOH. However, some unwanted etching of the rear p^+-layer of the solar cell may occur under the KOH etch. Therefore, a study was initiated to determine if a new p^+-layer needed to be formed by aluminum diffusion.

Prior to Al diffusion (and after KOH rear contact removal), cells were further cleaned with a deionized water dip followed by dilute hydrofluoric acid to remove the native oxide. This further cleans the cell and eliminates any residue or contamination. The following are high quality images (figures 10 and 11) were taken by an optical microscope at magnifications of 40x.

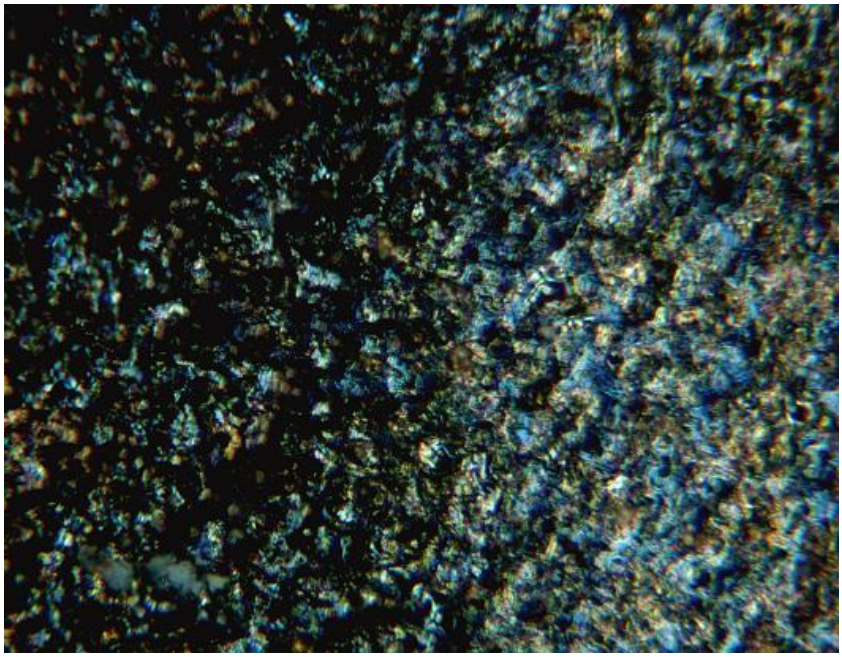

Figure 10: 40x microscope picture of bare Si after being etched by KOH.

As one can see, the surface is rough. First, the p^{+-}layer may no longer be present due to etching. The rough surface also indicates that it may be challenging to uniformly dope the rear of the solar cell by diffusion, although a rough rear silicon surface may aid light scattering. To study diffuse rear reflectors, a TiO_2 scattering layer was deposited on the rear surface of the silicon cell. This TiO_2 rear contact is shown in figure 11:

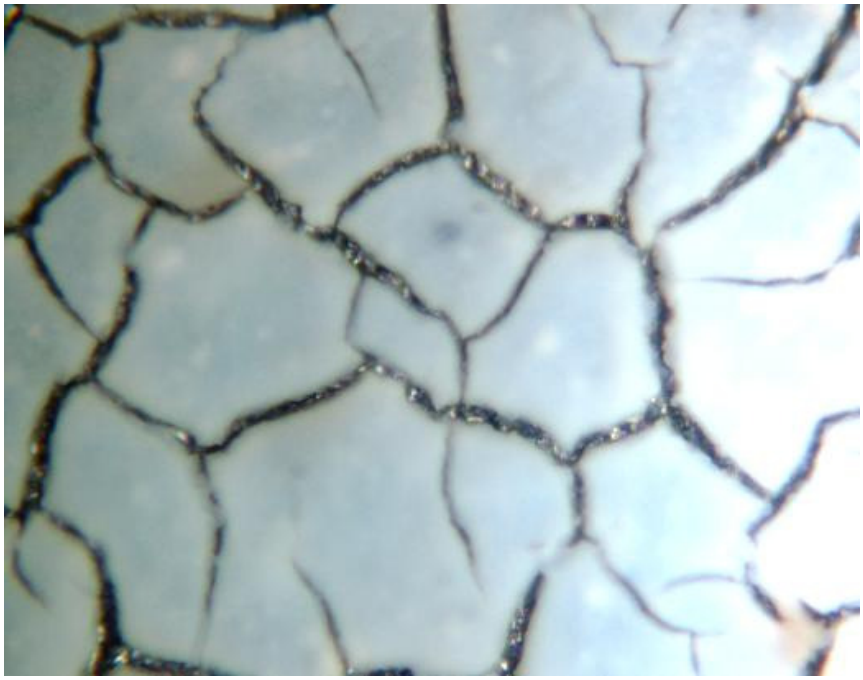

Figure 11: Si cell coated with TiO_2 scattering layer.

After examining this image, it was noticed that the TiO_2 had major cracks. In this application, cracks are not a problem as these may serve to allow a subsequently deposited rear metal contact to reach down and directly contact the silicon.

Also, Ag powder was used to test if the TiO_2 layer could be made more conductive. The Ag powder was tested separately to examine the properties under an SEM before and after heat

treatment in the furnace. Figure 12 shows the before picture; a sample of Ag particles full of spherical and cylindrical shapes. These do not necessarily reduce the reflectivity of the rear contact since silver is highly refractive.

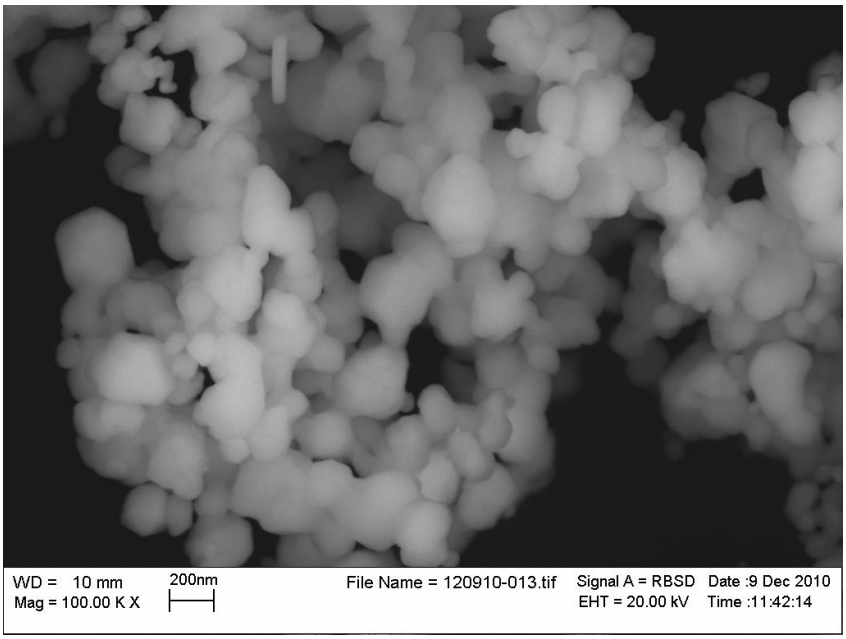

Figure 12: Ag powder before receiving heat treatment in a furnace.

Seeing this was encouraging in preparation to view the second Ag sample of heat treated powder. The powder was heat treated at 500°C for thirty minutes at a thirty minute increase to the set temperature and a two hour decrease back to room temperature. After being removed, the sample was viewed under the SEM. The results of this slide were even more encouraging, as much of the open area was fused together, leaving a minimal amount of openings along the surface. This can be seen in Figure 13 on the next page:

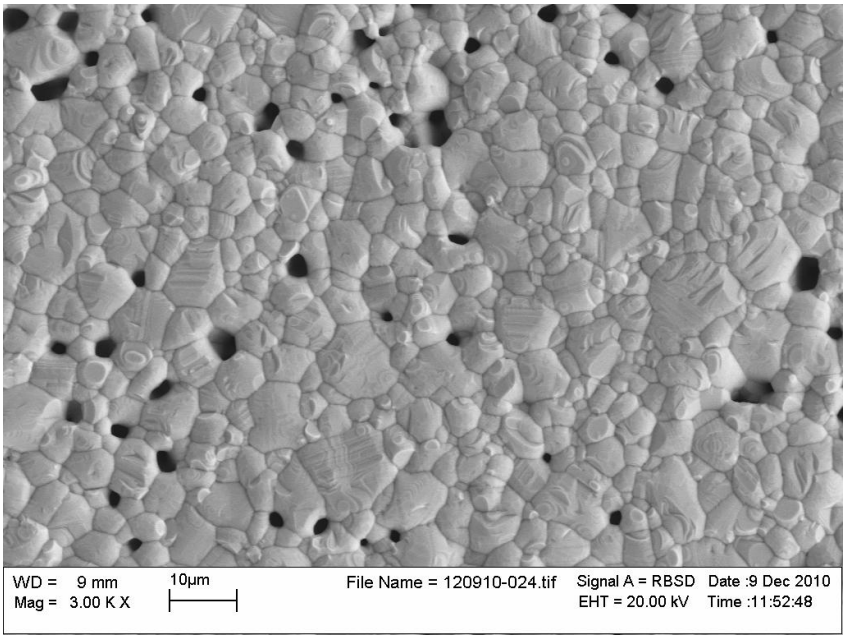

Figure 13: Ag powder after being receiving heat treatment.

3.2 Silver Paste Series

In order to create diffuse rear reflectors, various layer combinations were investigated. By omitting or using a combination of 40Å of evaporated Al as a contact layer, TiO_2 as a scattering layer, and a thin layer of silver paste as a back layer, several cells were tested. For the back layer, a coating of low V.O.C. waterborne Ag conductive ink was used. Care was taken to avoid shorting the cell by conductive materials depositing on the edges of the cell. If a conductive bridge is formed to allow charge to travel from the back of the cell to the front or vice versa, the cell will short and become unable to produce electrical power.

The results of the QE and solar simulations are presented in the chart shown in figure 15 as a function of rear contact configuration. Special attention was given to cell #4 due to its quantum efficiency in the red. This cell showed it is possible to improve upon the long

wavelength response of silicon solar cells by using diffuse rear reflectors. Comparing cell #4 to cell #1, an unmodified manufactured cell used as the control, one can see that the QE at 1100nm of cell #1 was 14%. By modifying the cell layers and creating a diffuse rear reflector, tests under the same conditions showed the QE at 1100nm to increase to 29.4%. The relative response is shown in figure 13. Other points of interest were centered on the overall maximum efficiency. Although this cannot be seen when comparing relative QE, the original peaks in the visible spectrum of both cells showed a peak of 86% QE in cell #1, whereas the peak in cell#4 is as high as 96% QE, a 5% QE increase from the control cell. This data proves that a cell with a diffuse rear reflector is able to trap and use more light than a standard Si cell. The differences in short wave length response can be attributed to damage and changes in the anti-reflection coatings due to processing.

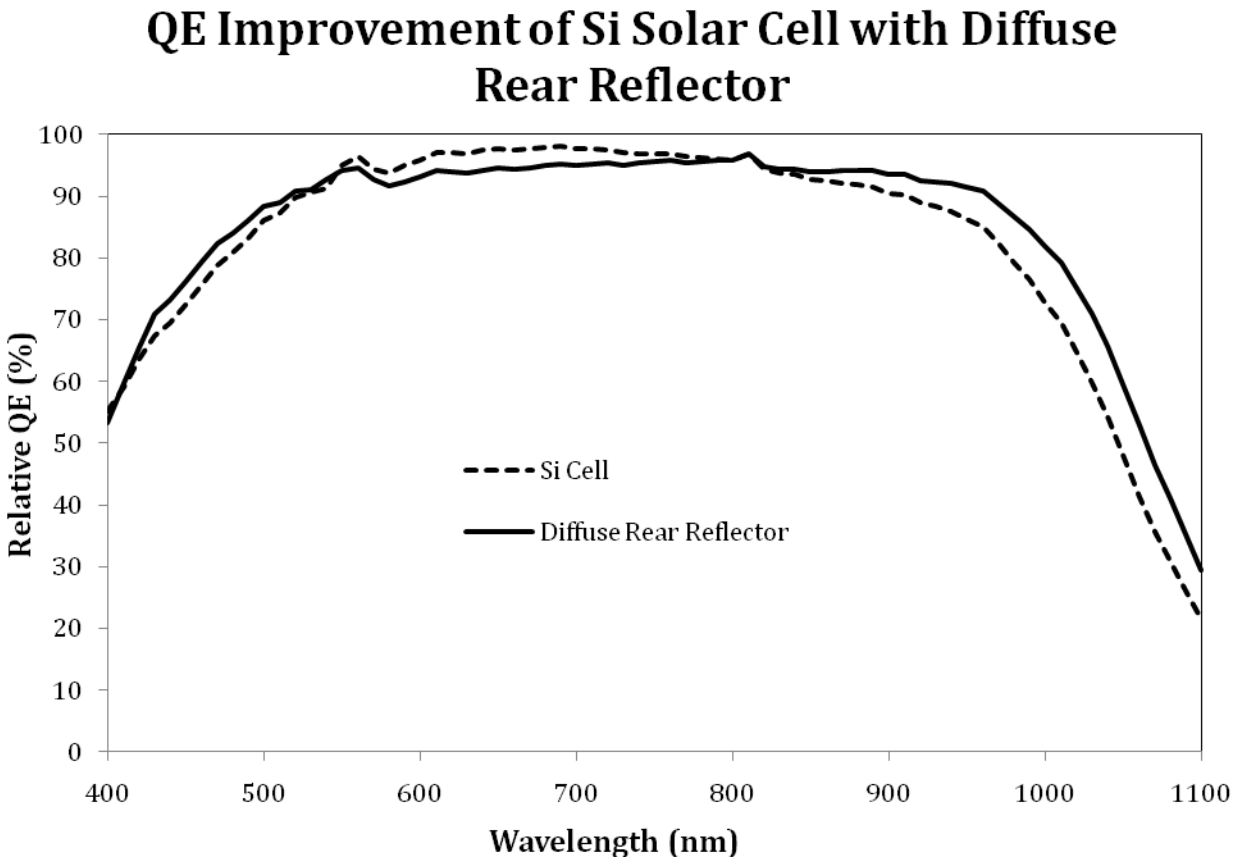

Figure 14: Comparison of Si solar cell with and without the presence of a diffuse rear reflector.

First and foremost, the presence of series resistance is unwanted and must be minimized. High resistance was found in most of the cells except cell #4 which omitted a contact layer. Voltages and currents throughout the cell also can be increased. Using cell #1 as the control, only two cells had a higher I_{SC} and V_{OC}. Cell #5 was the one cell that exceeded both of these, however it omitted a scattering layer. Cell #4 again exceeded the control by having a higher current.

The control cell had a high fill factor of 72%. It is important that all contact modifications maintain or improve upon this value. The closest achieved result was shown in cell #5, which omitted a scattering layer. According to the data; if the scattering layer is to be added, the fill factor decreases significantly. Also noticed is that if the scattering layer is to replace the contact layer, then the QE increases significantly. Thus, more conductive scattering layers are necessary. Alternatively, a better contact layer is needed.

Through many of the observations, it can be reported that cell #4 is the strongest cell in most of the variables. To improve the conductivity of this cell and maintain the optics, the most reliable suggestion is to change the material of the back layer. Al serves as a more electrically conductive material in both volume and weight. Using vacuum coating, Al was deposited onto comparable modified cells to test diffuse rear reflectors with an Al back layer instead of an Ag back layer. These cells were then tested under QE and solar simulation tests. As previously mentioned, figure 14 shows the results of the Ag back layered cells, while the results of the Al backing series is further reported in section 3.3.

Comparison In Solar Cell Layers						
	Cell #1	**Cell #2**	**Cell #3**	**Cell #4**	**Cell #5**	**Cell #6**
Contact Layer	STD	40Å Al	-	-	40Å Al	40Å Al
Scattering Layer	STD	-	-	TiO2	-	TiO2
Back Layer	STD	-	Ag Paste	Ag Paste	Ag Paste	Ag Paste
Voc (V)	0.6	0.57	0.61	0.53	0.6	0.55
Isc (A)	0.16	0.15	0.12	0.22	0.23	0.07
Jsc (mA/cm^2)	24.5	18.6	26	18.6	28.2	22.4
R at Voc	0.77	2.15	2.61	1.12	0.79	5.8
R at Isc	47.5	7.11	46.1	4.23	50.9	15.56
Fill Factor (%)	72	33	43.3	35	54.7	30.7
1100 QE (%)	14	10	12	29.4	6	8

Figure 15: A chart comparing several different cells and the results based on their compositions. Cell #1 was a standard (STD) cell which remains unmodified.

3.3 Aluminum Backing Series

As mentioned in section 3.1, after realizing the need for greater conductivity and better contacting, identical cells were modified with diffuse rear reflectors and Al vacuum coated back layers instead of Ag paste back layers. Several methods were used to eliminate the occurrence of series resistance and poor contact between the layers. The following chapter includes the discussion and description of a new set of methods that were used, including:

- Decrease in Al diffusion temperature to 300°C
- Increase of Al diffusion temperature to 900°C in order to drive the aluminum further into the silicon in an attempt to reestablish the p^+-layer.
- Using thin contact layers of semi-transparent platinum and titanium layers to eliminate contact resistance.
- Conduct a limited number of experiments on Raman-based spectral modification.

3.3.1 Temperature Changes

In an attempt to eliminate series resistance, a series of tests was initiated. The first cell in this series of tests was a silicon cell coated with a contact layer of 25Å of aluminum which was annealed at 500°C followed by a second Al layer of 250Å thick. These tests resulted in poor results, giving the first inclination that heat treatment serves as an inefficient environment for driving the aluminum into the silicon. Importantly, this test also indicated that the contact resistance rather than the diffuse rear reflector was the cause of the poor cell performance. The

temperature was increased to 650°C in order to raise the level of heat treatment to a more extreme temperature. Instead of the anticipated results of less series resistance, the results continued a trend of high series resistance due to a short and bad connection between layers. Also, the processing may have caused short circuits at the edge of the solar cell.

Upon gently cleaning the edges of the Si cell to remove the contamination and eliminate the bridge, results from the solar simulator again showed high resistance while also showing low voltage, current, and fill factor at an average of approximately 18.1%. Overall, the efficiency dropped significantly as well, averaging just 0.16%. The results continued to confirm the possibility that heat treatment was not as effective as originally thought. Lower temperature heat treatments were suggested by these results.

3.3.2 Addition of Materials

A new series of cells were created in which the contact layer was a dual layer of 8Å of platinum under 12Å of titanium. A scattering layer of 0.5g TiO_2 was then sprayed on top of the contact layer before again coating the cell with a 100Å layer of aluminum. The heat treatment after coating the back layer was lowered to 300°C and modified to add conductivity to the results as Ag paste was used to coat the back of the cell. The results proved to be better, as fill factor increased to average 24.18% and efficiency increased as well. However, the results were still not as high as needed. Comparisons showed between prior tests with Ag paste and the most recent tests gave further evidence for the need of minimal heat treatment only. The increase in performance was therefore a direct result of lowered Al annealing temperatures.

To prove this, a replica cell with a 15Å aluminum contact layer, a TiO_2 scattering layer, and 100Å layer back layer was created. The scattering layer was composed of 0.45g titanium dioxide and 0.05g Ag powder and heat treated at 100°C after application of the scattering layer to ensure fusion of the layers. The results for this cell proved that little heat treatment was necessary for the duration of creating diffuse rear reflectors. Results showed an extreme increase in performance. Considering the two important variables, the average cell efficiency was 5.09% and average fill factor was 29.12%. The one area where room for improvement existed was in quantum efficiency in the red, since the relative QE was only 16% in the red.

3.3.2.1 Introduction of Strong Raman Shifting Particles

Now having supporting evidence for the theory that heat treating the silicon cells was decreasing rather than increasing efficiency among other variables, the future of conducted experiments were not to be subjected to high temperature heat treatment. Over the period of several days, an etched silicon cell was coated with a 15Å layer of aluminum. A scattering layer of TiO_2 was then applied for added light scattering; however, the mix had more than just titanium dioxide. An addition of Ag powder was added for conductivity as well as particles capable of strong Raman shift as a new addition to the mix.

Five samples from a single large silicon solar cell were split into two batches; the first batch labeled as Batch A was sprayed with a TiO_2 and Ag powder mixture for light scattering and increased conductivity. The second batch was split into three cells, the first being a control of no spray. The other two were sprayed with a TiO_2 and Ag powder mixture as well; however, batch B added the ingredient of Raman shifting particles to the spray. All five cells were then

coated under the Denton with a 100Å Al back layer in addition to the 12Å Al contact layer coated before the cells were sprayed. Due to previous tests, these cells were not put under intense heat treatment, and again were subjected to 100°C to fuse the cell layers and allow for the cells to be put through two series of experiments.

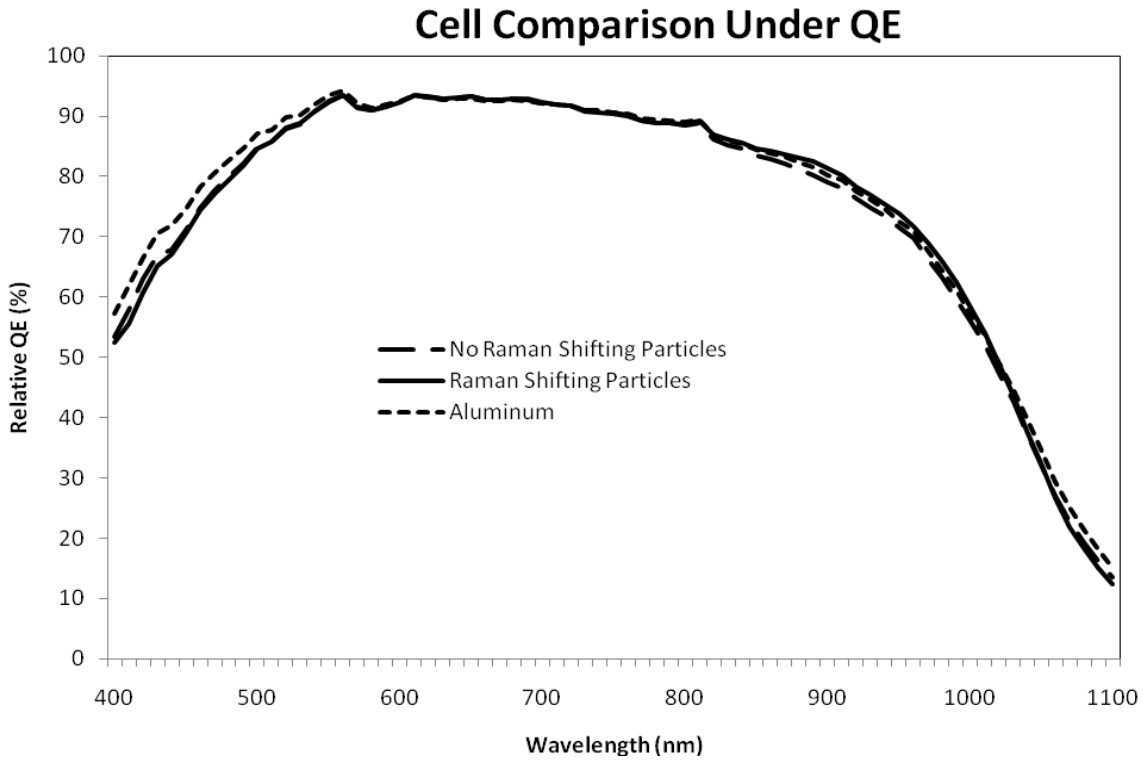

Figure 16: Comparison of three cells from the given batch. These cells showed a related QE showing little alteration between cells.

The first conducted test consisted of the normal set of quantum efficiency tests and solar simulations. Of all the past tests from the aluminum backing series, these tests were the most improved. Prior tests were receiving poor results of low efficiency in the red as well as high

amounts of resistance, most likely due to shorts or bad contact within the cell. Figure 16 above shows a comparison between three of these cells, including a cell with Raman shifting particles, a cell without them, and the aluminum only control cell.

The results suggest that when taking the relative QE, the greatest difference is evident between the wavelengths of 400-550nm and not towards the 1000-1100nm range. This ultimately shows that processing can alter the front anti-reflector coatings. The external quantum efficiency, which is always lower than the internal quantum efficiency, is the ratio of the number of charge carriers collected by the solar cell to the number of photons of a given energy that shine on the solar cell from the outside. In conclusion, these continued to be problems associated with contact resistance. In order to assess this situation, the scattering and back layers were held constant, while the contact layer was changed to titanium due to its greater oxygen resistance.

Although the QE results were not as impressive as desired, the solar simulation results were slightly better. First was cell #2 from batch A, whose scattering layer mixture did not include any Raman shifting particles. Also highlighted was cell #1 from batch B, whose scattering layer mixture did include Raman shifting particles. The comparison of these two cells is shown in figure 17 on the next page, while the comparison between each of these tests is interesting. The statistics of the batch A cell were far better than the statistics of the batch B cell. However, the overall shape of the curve was far better for the batch B cell. Fill factor of this cell was as high as 36.2% which was half-way to the desired goal of 70%. The cell also had an efficiency of 7.1%, a huge improvement from previous tests which resulted in several values less than 2%. Resistance was low as well; although the resistance at I_{SC} was high at 8.3, the open-circuit voltage (V_{OC}) was low at 1.9.

Comparing the batch B cell with that from batch A, fill factor decreased by 5% and efficiency decreased by 3%, while the current also decreased by 0.3 amperes and the V_{OC} resistance grew by almost 7 ohms. The I_{SC} resistance remained comparable; however the batch B cell had a much better I-V, showing less relative current loss than the batch A cell. It is safe to assume that the addition of Raman shifting particles had a positive effect on the efficiency of the cell and reduced current losses. In general, the results of both of these cells showed improvement; however more improvement is always desired and needed. Efforts are underway to obtain fresh un-coated solar cells so that contacts will not be etched away. These would likely not suffer from the same contacting problems as reported above.

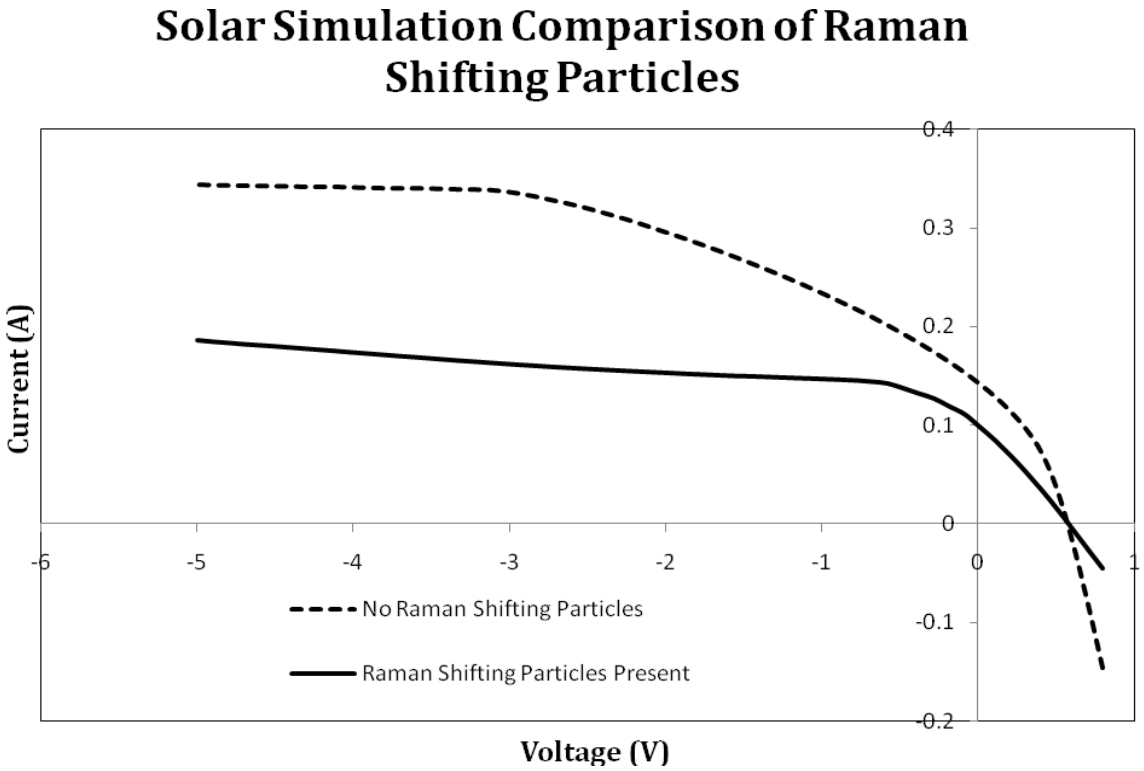

Figure 17: Solar simulation of a silicon cell containing Raman shifting particles within its scattering layer.

3.4 Titanium Contact Series

The continued need for contact between spectral layers as well as the increased absorption of photons resulted in the use of titanium as a contact layer. A silicon cell was coated with 12Å of Ti before being coated with 150Å of aluminum. After coating, the cell was immediately tested and measured under QE and solar simulation. Results were recorded as the cell then proceeded to undergo a heat treatment of 100°C in which when concluded, was again tested and measured under solar simulation before being placed back in the furnace for a heat treatment of 300°C. After another testing and recording of results, one final heat treatment of 500°C was undergone as well as one final series of tests. The results are as shown in figures 18 and 19.

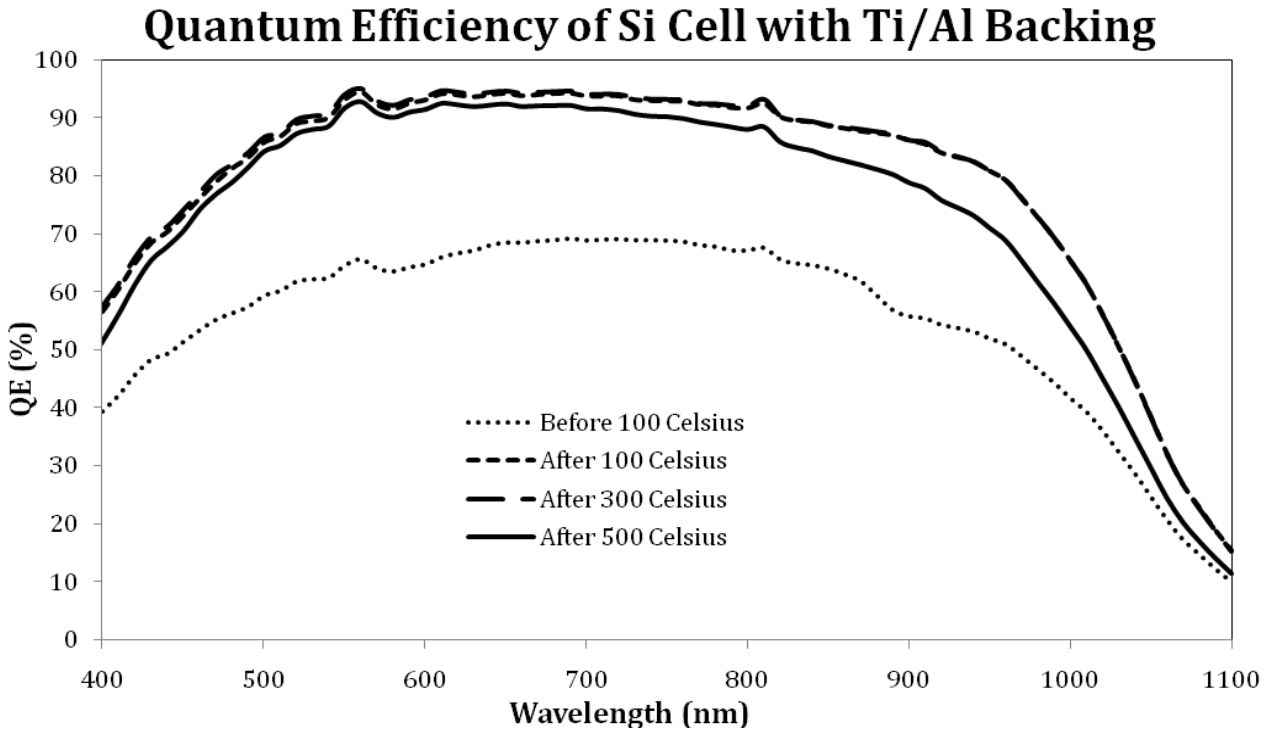

Figure 18: Quantum efficiency of a coated Ti contact layer/Al black layer silicon cell at different temperatures of heat treatment.

In figure 18, it was noticed that the overall QE of each successive test increased in both overall efficiency, as well as QE percentage in the red. This pattern held true until measurements were taken after the 500°C heat treatment, in which the percentages and values dropped slightly. Figure 19 shows this same pattern as well; an increase in values and data until the 500°C treatment shows damage to the cell. Combing the previous heat treatment tests from sections 3.3 and 3.4, it could be concluded that heat treatments do indeed aid the overall efficiency of the cells. However, if the heat goes over a threshold of ~300°C, the cell will decrease in efficiency. This information was applied to the next test, in which two cells were coated with the same layers; a 12Å Ti contact layer and a 150Å Al back layer. However, an additional layer of TiO_2 and Ag powder were added to the mix as well, and tested under similar conditions.

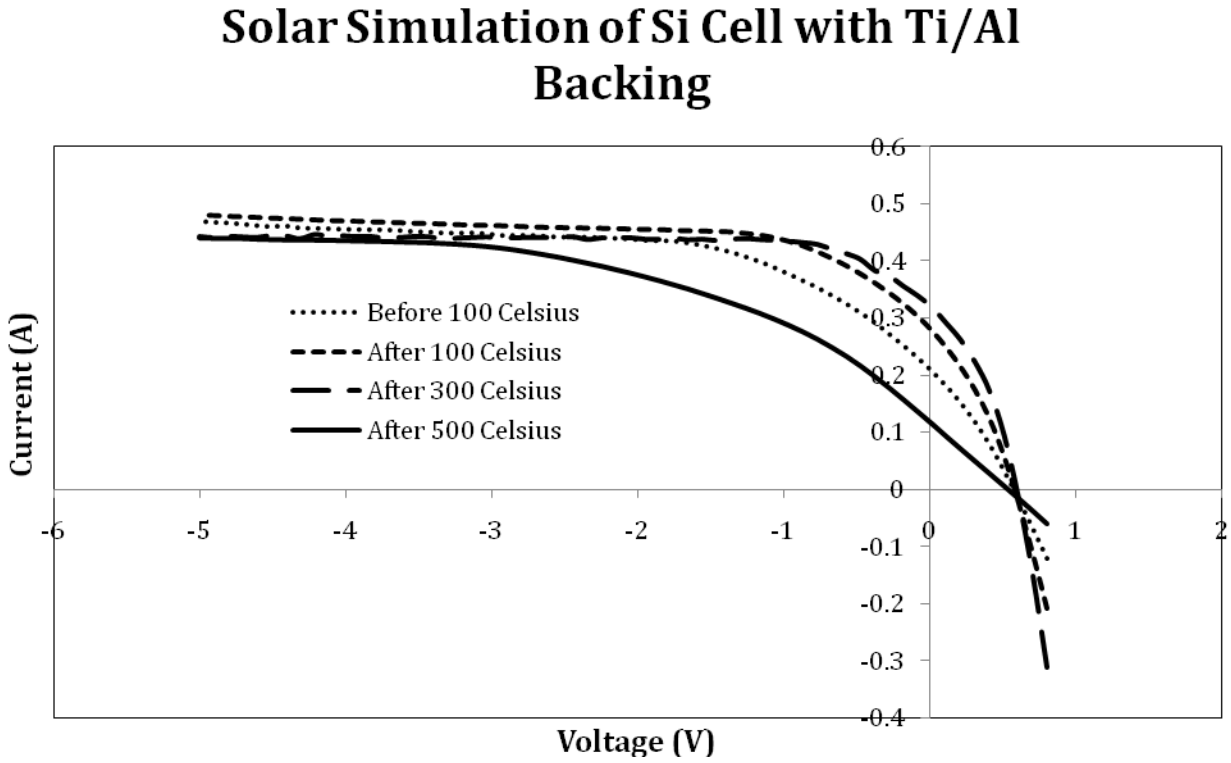

Figure 19: Solar simulations of a coated Ti contact layer/Al black layer silicon cell at different temperatures of heat treatment.

3.4.1 Titanium Results

In testing the efficiency of titanium and as previously mentioned, a scattering layer was added to the two cells to test the efficiency of them. The objective was to fuse the layers and allow for the titanium to serve as a blocking mechanism for the prevention of oxide formation. After heat treatment, the cells were tested under the normal conditions of quantum efficiency and solar simulation. As seen in figure 20, the comparison of spectral layers shows that the efficiency of the titanium coated contact layer is fairly similar to the other cells; one with a scattering layer, and one with no modifications at all. It also shows that at 1100 QE, the cell with no scattering layer has a lower QE than the cell with scattering layers.

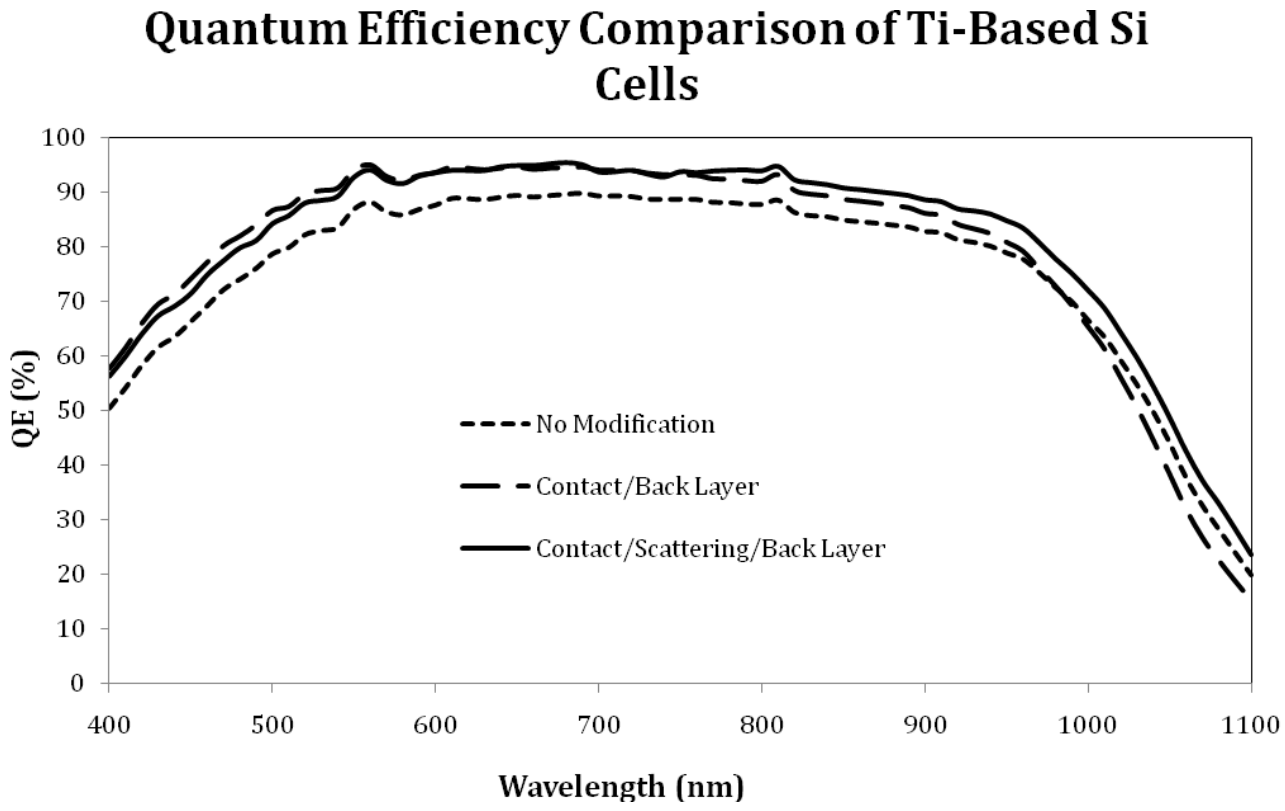

Figure 20: Comparison of spectral layers showing the efficiency of a titanium contact layer.

IV. Conclusions

4.1 Cell Comparison

Taking into consideration the many cells that have been created, the spectral layer combinations can be grouped into differences in each respective layer. In regards to the three layers discussed throughout this thesis, each layer has been over a range of preparation conditions. The back layer has been varied between aluminum and Ag paste. It is known that aluminum for its high conductivity is also reflective. Ag paste is even more conductive and has greater reflectivity than aluminum. It was used as the back layer for the most efficient cells found by this work. More tests will confirm which material is a better material to use for the back layer.

The scattering layer throughout was based as a TiO_2 mixture. These mixtures included subtracting TiO_2 to add Ag Powder and/or Raman shifting particles, or adding more TiO_2 to create a greater amount of mixture. As seen in the results, using TiO_2 as a diffuse rear reflector almost doubled the long wavelength quantum efficiency of a commercial cell with an aluminum paste contact. Further experiments using these combinations will prove the necessity for greater conductivity, such as the use of Ag powder, as well as increased light scattering, such as the Raman shifting particles.

In this work, the contact layer proved the most problematic area. Failing to dope a sample allows for a decrease in electrical properties and efficiency in the cell. Therefore, both aluminum and titanium were used as a dopant material; however it was the amount of dopant and the amount of heat treatment that had the greatest effect. Several tests were done without heat treatment, while others were done with heat treatments as high as 500°C. Overall, a trend formed

as heat treatment mattered depending on the contents of the cell. It was discovered that additives to the scattering layer changed the color from a lighter blue to a dark purple after heat treatments. It was also noticed that contact layers strengthened as heat treatment approached 300°C, but decreased as heat treatment continued. Experimenting more with different types of dopants as well as different amounts of heat treatments will provide increased data to form even greater contact layers.

4.2 Improvements and the Future of Diffuse Rear Reflectors

The creation of diffuse rear reflectors can continue if these three layers are created in such a way that they aid each other in increasing all of the necessary components of an efficient solar cell, while decreasing negative parameters as well. These include non-fusion of layers, shorts, series resistance and several other parameters. In conclusion, the diffuse rear reflector works to improve the long wavelength response of solar cells. However, complications related to the removal of contacts from commercial solar cells lead to many difficulties associated with contact resistance.

The best achieved overall quantum efficiency seen here for a silicon cell with a TiO_2 diffuse rear reflector case was 29.4% at 1100nm in the red. Although the existence of series resistance in many samples was present, this resistance is the result of process related problems including unwanted deposits. The first solution is always to consider impurities on the sample. Although the utmost care is taken to properly clean and prepare every sample before they are sprayed, coated, or heat treated, many samples have already been contaminated during manufacturing. Since the samples are exposed during the fabrication process, surfaces and

interfaces are more likely to be contaminated. Ongoing work includes the complete re-engineering of processes that produce rear contacts so that the diffuse rear reflector is applied to the silicon wafer after the rear p^+-layer formation.

References

1. Pancaldi, Giuliano. *Volta: Science and culture in the age of enlightenment.* Princeton University Press, 2003.

2. Green, Martin A. *Photovoltaic Principles*. Special Research Centre for Third Generation Photovoltaics, University of New South Wales, Sydney 2052, Australia. Physica E 14 (2002): 11-17. Print.

3. A. Stoletow (1889). (in Russian) *Journal of the Russian Physico-chemical Society* 21: 159.

4. "The Nobel Prize in Physics 1921". Nobelprize.org. Retrieved 23 December, 2010. http://nobelprize.org/nobel_prizes/physics/laureates/1921/

5. Perlin, John. *"The Silicon Solar Cell Turns 50"*. National Renewable Energy Laboratory. (2004). Retrieved 22 December, 2010.

6. Navneet Gupta and S. K. Tiwari. *A textbook of Engineering Physics.*

7. Taylor, John R., Chris D. Zafiratos, and Michael A. Dubson. *Modern Physics for Scientists and Engineers*. Upper Saddle River: Prentice Hall (2004): 127-130. Print.

8. Wikipedia: Theory of Solar Cell. <"http://en.wikipedia.org/wiki/Theory_of_solar_cell>. Author: GianniG46. Retrieved 4 January, 2011.

9. Kittel, Charles. *Introduction to Solid State Physics – 8th Edition.* Page 429. Hoboken, New Jersey. John Wiley & Sons Inc., 2005.

10. "Solar cell: Encyclopedia II - Solar cell – Theory." Global Oneness. <http://www.experiencefestival.com/a/Solar_cell_-_Theory/id/5376728>. Retrieved 13 January, 2011.

11. "Refractive Index." <http://www.britannica.com/EBchecked/topic/495677/refractive-index>. Encyclopedia Brittanica. Retrieved 9 May, 2011.

12. Green, M.A. "*Third Generation Photovoltaics*." Springer-Verlag. (2003).

13. Fahrenbruch, Alan L. & Bube, Richard H. *Fundamentals of Solar Cells: Photovoltaic Solar Energy Conversion.* New York, New York. Academic Press, 1983: 95-98. Print.

14. K. Winz, C.M. Fortmann, Th. Eichkoff, C. Beneking, H. Wagner, H. Fujiwara and I. Shimizu, *Sol. Energy Mater. Sol. Cell* **49** (1997): p. 195. Print.

15. P. Lee, J. Shank, K. Magsi, Y. Kang, C.M. Fortmann: "*Optical Layers and Materials for Next Generation Solar Cells.*" 2011. **See Appendix 1**

16. Glicksman, Martin Eden. "*Diffusion in Solids*". Hoboken, New Jersey. John Wiley & Sons, 2000.

17. Borg, Richard J. & Dienes, G.J. "*An Introduction to Solid State Diffusion*". London. Academic Press, Inc., 1988.

18. Rampf, Gerald & McCafferty, Robert: "Devising an APC strategy for metal sputtering using residual gas analyzers". <http://www.micromagazine.com/archive/02/07/rampf.html>. Micromagazine.com. Retrieved 12 May, 2011.

19. Newport: "Solar Simulators". <http://search.newport.com/i/1/q1/Products/q2/Light+Sources/q3/Solar+Simulators/x1/pageType/x2/section/x3/chapter/nav/1/>. Retrieved 18 January, 2011

20. Wikipedia: "Quantum Efficiency". <http://en.wikipedia.org/wiki/Quantum_efficiency#cite_note-1>. Retrieved 14 December, 2010.

21. G. C., B. C. Chakravarty, and S. N. Singh. "Dopant Profile Analysis of Boron in Solar Grade Poly- and Single- Crystalline Silicon." *Applied Physics Letters* 38.10 (1981): 815. Print.

22. Robert C. Weast, Editor. *Handbook of Chemistry and Physics*. CRC Press, Boca Raton, FL. 1979.

Appendix 1

OPTICAL LAYERS AND MATERIALS FOR NEXT GENERATION SOLAR CELLS

Ping Lee[1], Jason Shank[1], Komal Magsi[1], Yeona Kang[1], C.M. Fortmann[1, 2]

1. Materials Science and Engineering Department, Stony Brook University, Stony Brook, NY 11794-2275
2. Idalia Solar Technologies LLC, 270 Lafayette St. Suite 1402 New York, NY 10012

Abstract

Layers that enhance light scattering and Raman-scattering-based spectral modification for solar cell applications were investigated. Titanium-oxide based rear diffuse reflectors were found to increase the long wavelength response of crystalline solar cells. Also particle within the Titanium-oxide produce a far greater Stokes and anti-Stokes shift when compared to bulk crystal counterparts. The anti-Stokes to Stokes shift ratio in these particle systems is also greater and increased with increasing probe or bias light intensity. When applied to solar cells these layers extend the red response and thereby increase the overall performance.

Introduction

Over thirty years of solar cell advancement provides a vista to new strategic technologies for greater photovoltaic solar energy production. This work examines the increased performance and reduced cost made possible by front and rear mounted spectral modification layers for use with a variety of solar cell platforms [1]. Since, photovoltaic cells convert a narrow portion of the sun's energy to electrical power any means that broadens the response without consuming useful light will lead to improved efficiency. Front mounted systems that down convert UV light and rear mounted systems that up convert light are sought. Raman up converters incorporated into the diffuse rear reflector offer a means by which to scavenge unused light and convert it into light of sufficient energy to broaden the conversion range. Raman scattering is an intrinsically weak phenomena commonly used for material characterization. The challenge is to increase the shift to levels that result in significant improvement of solar cell performance. On the other hand Raman scattering can account for significant loss (~~25%) in long distance fiber optic communication. Raman-scattering (Stokes and anti-Stokes shift) based up-conversion characterized by: energy and momentum conservation was investigated because it has no minimum photon flux requirement and when positioned at on the back of the solar cell minimal parasitic light absorption.

Experiment

Titanium oxide and Zirconium oxide/Titanium oxide mixed particles films of various thicknesses were prepared and applied to the back of commercial silicon solar cells (after removal of the as delivered rear contact paste). Similar films were also deposited onto glass slides using a standard hobby spray apparatus. To facilitate film spraying nanoparticles were

mixed with isopropanol and water. The films were then annealed at 500 ^{o}C for one hour and slow cooled. Film coated glass slides were placed in front of the reference silicon solar cell (~ 16% efficient under AM 1.5 illumination) and the quantum efficiency measured using a Newport Oriel quantum efficiency system with and without bias light. These same films were also placed in front of a standard germanium reference photovoltaic cell for visible and IR spectral transmission measurement. A ~1.5 watt CW visible light laser was used for the bias light cases.

The Raman shifts of bulk crystal and nanoscaled ($1\ \mu m$) crystalline particles systems known to have large Raman shifts were measured using a Thermo Nicolet Almega dispersive Raman Spectrometer. Figure 1 shows the response of silicon nanoparticles (100 nm range). It was found that the Raman shift to the Anti-Stokes to Stokes ratio of the particle systems were greater than their bulk crystal counterparts. Relatively large Raman shift for particles as compared with bulk crystal was also found in visible light transparent particle systems. In all cases the Anti-Stokes to Stokes ratio increased with increasing probe and with bias light.

Results

A titanium oxide diffuse rear reflector that increases the quantum efficiency at $\lambda = 1{,}100\ nm$ as compared to the aluminium pastes typically used on commercial crystal silicon solar cells by 25% as seen in Fig. 2. These difference rear scattering layers enable the use of flat minimal area front contacts that can decrease the front surface recombination by more than a factor of 2 when compared with a triangular light scattering front surface structure.

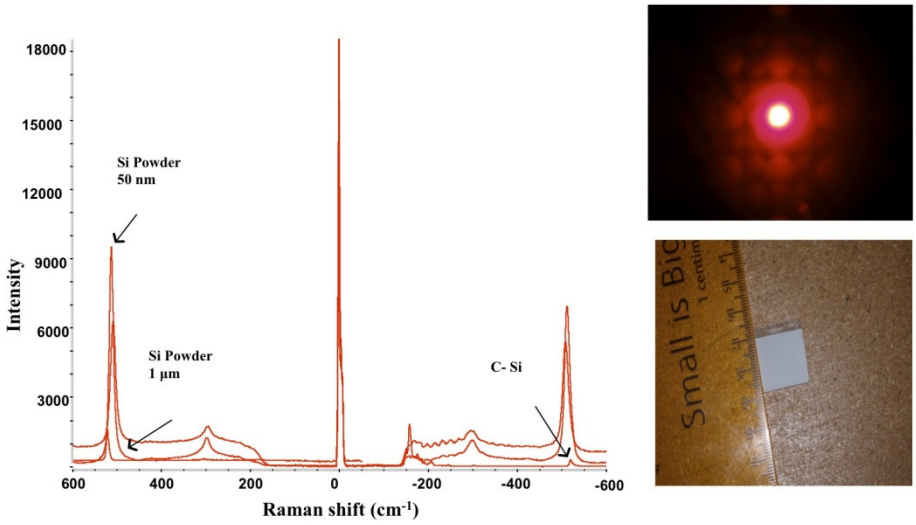

Figure 1. Shown are the Raman spectra of crystalline and nanoscaled particle silicon. Similar results were obtained for a number of visible light transmitting particles. Inset shows the spread of laser pointer light by a thick titanium oxide-based film.

The Raman Shifts of the particle systems tended to produce both the larger amplitude shifts as well as the larger Anti-Stokes to Stokes ratios when compared to the bulk crystal forms of the same materials. The Anti-Stokes to Stokes shift also increased with increasing probe beam intensity and it also increased with bias light illumination. The results are consistent with a phonon transfer mechanism in which a phonon generated by a Stokes shift event leaves behind a long-enough lived phonon to contribute to an anti-Stokes shift (energy increasing) event. Careful analysis based upon a diffusion in energy predicted over ~30% of the Raman shifted light will be towards higher energies (space limitation preclude calculation inclusion in this work) where the photon could contribute to power generation.

Various films comprised of Titanium oxide particles or Titanium the Raman shifting particles on glass substrates were placed in front of a standard silicon reference cell. The back scattering of the light reduced the overall quantum efficiency of the solar cell as seen Fig. 3 with increasing film thickness. When the same films were placed in front of the germanium solar cells the relatively featureless response of the germanium photovoltaic cell reveals a spectrally flat decrease in solar cell quantum efficiency indicating no spectral bias in either film transmission or film light scattering.

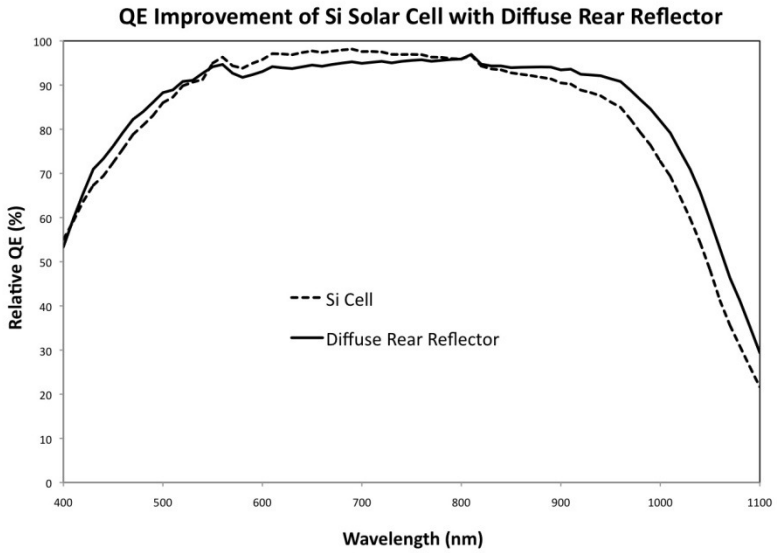

Figure 2. Comparison of a commercial solar with the as-delivered back contact and a diffuse Titanium-oxide based rear reflector (applied after removal of the as-delivered back contact).

Light transmission of the various films are spectrally flat the QE curves were normalized with respect to the response without film cover. The resultant plot is also shown in Fig. 3. Figure 3 shows that with strong Raman scattering particles and with light bias there is a distinct increase in the QE near the band edge of silicon.

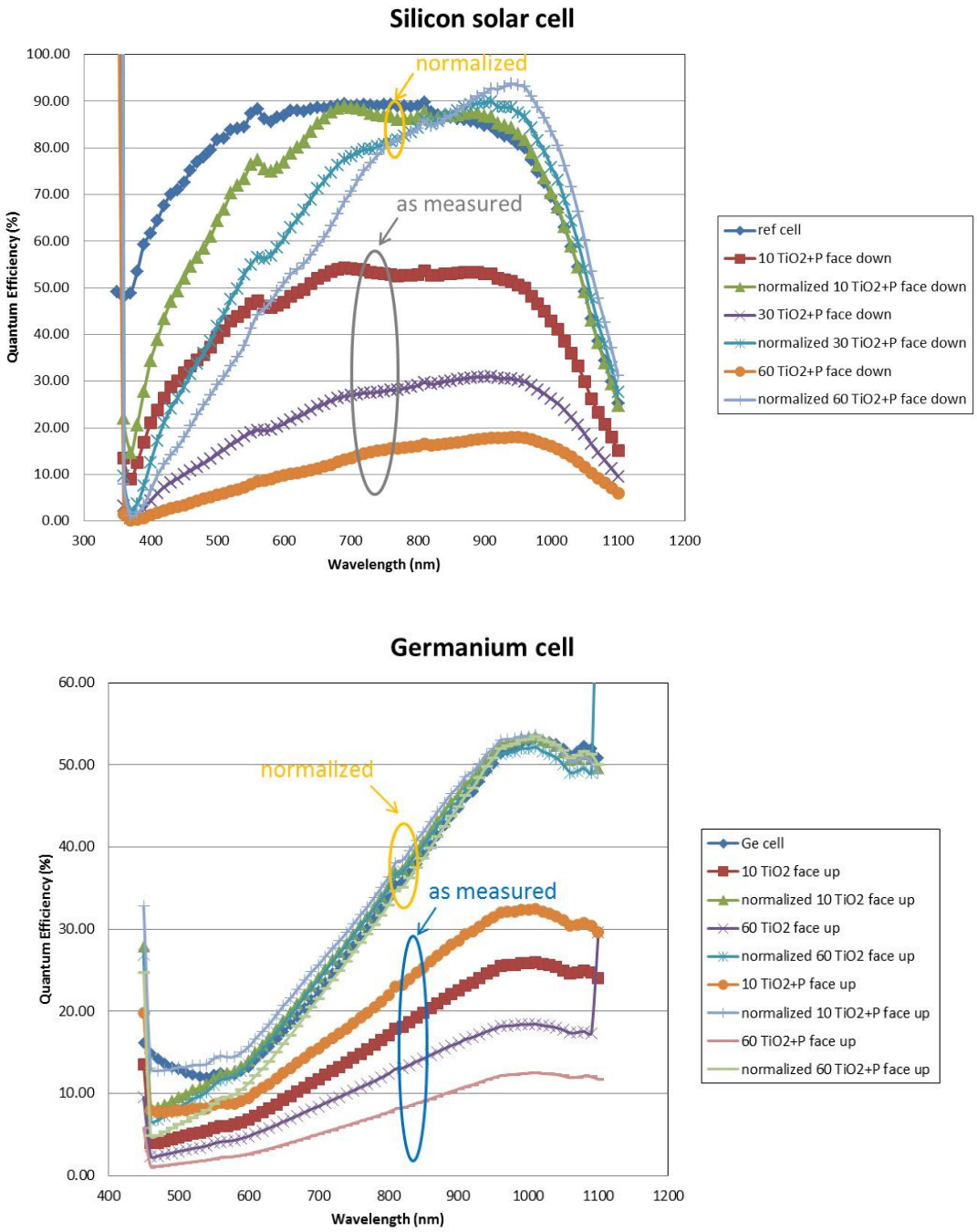

Figure 3. Shown is the quantum efficiency of standard silicon solar cell (top) in which various thickness titanium-oxide – based films (with and without Raman shifting articles as indicated) on glass substrates was placed in front (illuminated) of the solar cell. The graph at the bottom shows the performance of a germanium photovoltaic with the same layers in front.

Discussion

Diffuse rear reflectors offer the advantage of scattering light to sufficiently large angles so as to increase probability of total internal reflection at the front surface and therefore much longer light path lengths within the solar cell absorber layer when compared to a simple mirror like rear reflector. To obtain large scattering angle within a high index solar cell (refractive index of silicon > 3.4) the diffuse rear reflector must also have a large refractive index as previously noted by Winz *et al*. [1]. This work reports on a sintered rear reflector capable of increasing the long wavelength response by 25%. Interestingly, while diffuse rear reflectors increase performance, diffuse front reflectors decrease performance by > 40% mostly due to the large amount of light scattered and/or reflected out of the front of the solar cell (see Fig. 3).

Raman-scattering is an extensively used analysis tool. Also, Raman-scattered light can account for upwards to 25% of the transmitted light in long distance fiber-optic communications. However, until now Raman scattering has not been utilized to modify the solar spectrum for improved solar cell performance; perhaps because it would appear unlikely that the thin solar cell layers could generate the path lengths necessary for significant Raman scattering probability. Nonetheless, extremely long path lengths are possible in thin diffuse layers. Figure 1 (inset) shows a thin-film TiO2 layer used in the experiments described above being illuminated by a laser pointer. It is clearly seen that light spreads to distances beyond 1 cm.

Taking this 1 cm value as the route mean square distance, $\langle R \rangle$, which can be defined by standard diffusion practice as $\langle R \rangle^2 = \lambda^2 N$ where λ is the average jump length, and $N$is the number of diffusing particle jumps (here photon scattering events). Taking the scattering particle grain size as the jump length ($\sim 250\ nm$) the travel distance a photon makes through the material as it diffuses to the absorbed distance of 1 cm is a remarkable 400 m (since $\langle R \rangle^2 / \lambda = N\lambda$, the travel distance). Therefore, it is conceivable that Raman up conversing is responsible for the inverse rear when the Raman shifting particles are added to the TiO_2 films.

Conclusions

Light scattering in thin film particle systems has been shown to offer pathways to greater photovoltaic performance. Near-index matched rear reflector systems offer increased current without detrimental surface area increase. The Raman scattering and the anti-Stokes-to-Stokes ratio is greater than that of bulk crystal counterparts and these further increase with increasing probe beam or bias light intensity. Spectral modification via these systems is capable of significantly enhancing solar cell performance.

Acknowledgment

The authors thank Eric Laufer and Idalia Solar Technologies for partial support. We also thank: NYS Sensor Center for Advanced Technology and NYS SPIR program.

References

1. K. Winz, C.M. Fortmann, Th. Eichkoff, C. Beneking, H. Wagner, H. Fujiwara and I. Shimizu, *Solar Energy Materials and Solar Cells*, **49**, 195 (1997).